of the scattered proton. [The imaginary term in the potential, as discussed by Heckrotte (H 56), corresponds to the absorption being spin-dependent.]

A strong maximum in the polarization at 20°, a negative maximum at 14°, and another maximum near 10° was found. The locations of these peaks were not sensitive to the value of U_i. In the scattering cross section a minimum at 14° and a maximum at 18° was predicted. It must be remembered in applying these calculations, that they were made for silver bromide which represents only 76% of the cross section in emulsion.

The use of diluted emulsion for experiments on polarization by scattering in emulsion might have great advantages. An obvious one is that the Coulomb scattering is reduced. Another could be that at some practical ratio of gel to halide, the average polarization on scattering might pass through a maximum. These possibilities have not as yet been studied in detail.

A recent important application of emulsion as a polarization detector has been made by Maloy *et al.* (M-S 60.1). The polarization of protons recoiling from the reaction $\gamma + p \rightarrow \pi^\circ + p$ was measured.

8.4 Multiple Scattering

The change in direction of motion, θ, that a particle experiences in penetrating a thickness, t, of matter is a random variable. The probability distribution of θ is affected by the nature of the particle and its velocity as well as by the composition of the scattering material. The average value $\langle\theta^2\rangle$ of θ^2 increases in close proportion to t. A variable

$$\theta_s^2 = \frac{d\langle\theta^2\rangle}{dt} \tag{8.4.1}$$

which depends on the kind of particle and the scattering material, is a parameter measuring the scattering. It is the same as the θ_s^2 introduced by Rossi (R 52). As long as the scattering consists of many small deflections θ_s is sufficient to describe it, for then, in virtue of the Central Limit Theorem, (C 46), the resultant distribution of angles will be Gaussian.

For small thicknesses of matter, however, the number of deflections may not be large, so that the form of the elementary law of scattering affects the resultant distribution. For the present, the energy loss in the absorber is neglected.

As long as θ_s is small, the mean square *projected* angle $\langle\phi^2\rangle$ is related to θ_s^2 about as follows:

$$\frac{d\langle\phi^2\rangle}{dt} \approx \frac{1}{2}\theta_s^2 \tag{8.4.2}$$

Assuming θ_s to be roughly constant this can be integrated to give:

$$\langle\phi^2\rangle = \frac{\theta_s^2}{2}t \tag{8.4.3}$$

This implies that the average projected angle of deflection of a particle also varies with the square root of the thickness of matter penetrated.

The Coulomb scattering of a charged particle is caused by the same electric fields that induce bremsstrahlung (Chapter 5 in Volume II). For an absorber thickness comparable to the electron radiation length, and for $\beta \approx 1$, the two effects can be directly related (R 52). Under these conditions:

$$\theta_s \approx \frac{21.2z}{p\beta x_0^{1/2}} \tag{8.4.4}$$

where x_0 is the radiation length, and p is in Mev/c. This is a valid approximation only when the absorber thickness is great, so that a large number of scattering events are represented in the net deflection of a single particle. For Eq. (8.4.4) to be valid it is also required that the particle energy be high. This insures that θ_s be small. Moreover, the particle must not interact strongly with atomic nuclei. For these reasons the expression is useful only for high energy μ mesons. Because of their rapid rate of energy loss by radiation, electrons seldom penetrate more than a few radiation lengths.

When strongly interacting particles penetrate a large thickness of matter, the conditions leading to the Central Limit Theorem are not satisfied. The occasional large deflections that occur both from Coulomb and non-Coulomb interactions may dominate the observed angular distribution. Whereas the root-mean-square multiple scattering angle increases only with the square root of the absorber thickness, the number of particles that penetrate the absorber without suffering a large deflection falls exponentially with its thickness. (This assumes that the particle velocity is so high that its energy is not appreciably changed in the absorber.) After a beam penetrates a distance equal to a mean free path for nuclear interaction, a large fraction of the particles no longer will lie in the Gaussian distribution.

This is illustrated by Fig. 8.4.1 which shows the projected angular distribution of a beam of negative pions. The beam originally had a negligible angular dispersion and its momentum was 700 Mev/c. The angular distribution after it penetrated to a depth of 20.3 cm in a large stack of emulsion is shown. This distance is somewhat more than half the

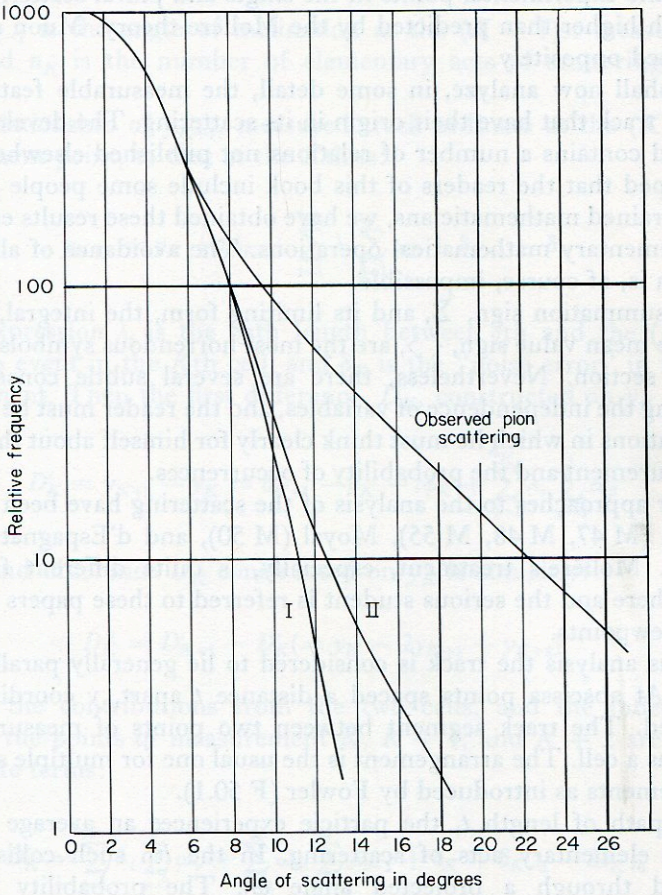

FIG. 8.4.1. Observed multiple and plural scattering of pions compared with the Molière Theory.

mean free path for a non-Coulomb interaction so a considerable fraction of the surviving particles will have been scattered through a large angle.

The curves shown were calculated from the Molière theory (see Section 8.8), which gives the total Coulomb scattering in the screened electric field of a point nucleus. Curve I is the Gaussian part of the

Molière scattering alone. It represents the true *multiple* scattering. Curve II includes the effect of single and plural scattering in the Coulomb field according to Molière. This part of the curve is affected by the elementary scattering law, and by the approximations of his theory. One can see that, owing to the strong interaction between pions and atomic nuclei, the experimental points in the single and plural scattering region lie much higher than predicted by the Molière theory. Muon scattering is affected oppositely.

We shall now analyze, in some detail, the measurable features of a particle track that have their origin in its scattering. The development is new and contains a number of relations not published elsewhere. Since it is hoped that the readers of this book include some people who may not be trained mathematicians, we have obtained these results employing only elementary mathematical operations. The avoidance of all abstract notation is, of course, impossible.

The summation sign, Σ, and its limiting form, the integral, $\int$, along with the mean value sign, $\langle\ \rangle$, are the most horrendous symbols required in this section. Nevertheless, there are several subtle considerations regarding the independence of variables, and the reader must be prepared for situations in which he must think clearly for himself about the process of measurement and the probability of occurrences.

Other approaches to the analysis of the scattering have been made by Molière (M 47, M 48, M 55), Moyal (M 50), and d'Espagnat (D 51.1, D 52.1). Molière's treatment, especially, is quite different from that offered here and the serious student is referred to these papers to obtain other viewpoints.

In this analysis the track is considered to lie generally parallel to the x axis. At abscissa points spaced a distance t apart, y coordinates are measured. The track segment between two points of measurement is known as a cell. The arrangement is the usual one for multiple scattering measurements as introduced by Fowler (F 50.1).

In a path of length t, the particle experiences an average number, $N\sigma t$, of elementary acts of scattering. In the lth such collision it is deflected through a projected angle ω_l. The probability that the scattering angle, ω, is in the interval $d\omega$ is $\rho(\omega)d\omega$. Now we define $\langle\omega^2\rangle \equiv \int \omega^2\rho(\omega)d\omega$. The quantity $N\sigma$ above is the product of the number N of scattering centers per unit volume and the total scattering cross section, σ. Then $\langle\phi^2\rangle = N\sigma t\langle\omega^2\rangle$. This is the mean square angular change of the projected particle direction in one cell length.

We shall make the small-angle approximation in which $\sin\omega$ is taken equal to ω. This introduces no significant error in the analysis of the scattering of fast particles.

At the Kth abscissa point along the track, let ϕ_K be the projected angle of inclination of the track to the x axis. Then

$$\phi_K = \phi_{K-1} + \sum_{l=1}^{n_{K-1}} \omega_l \tag{8.4.5}$$

where ϕ_{K-1} is the angle of inclination at the $(K-1)$st measurement point, and n_K is the number of elementary acts of scattering in the Kth cell.

The relationship of y_{K+1}, measured track ordinate at the $(K+1)$th measurement point, to that at the Kth is:

$$y_{K+1} = y_K + t\phi_K + \sum_{j=1}^{n_K} \lambda_j \sum_{\beta=1}^{j} \omega_\beta + \delta_{K+1} - \delta_K \tag{8.4.6}$$

In this expression λ_j is the path length between jth and the $(j+1)$st scattering event in the Kth cell, and δ_K is the "noise error" in the Kth measurement. Then the first difference, D'_K, constructed on y_K is:

$$D'_K \equiv y_{K+1} - y_K = \delta_{K+1} - \delta_K + t\phi_K + \sum_{j=1}^{n_K} \lambda_j \sum_{\beta=1}^{j} \omega_\beta \tag{8.4.7}$$

The second difference D''_K constructed on y_K is similarly:

$$D''_K = D'_{K+1} - D'_K (= y_K - 2y_{K+1} + y_{K+2})$$

When the contributions from the two cells, and the independent errors at the points of measurement K, $K+1$, and $K+2$ are written as separate terms:

$$D''_K = \sum_{i=1}^{n_{K+1}} \lambda_i \sum_{\gamma=1}^{i} \omega_\gamma + \sum_{m=1}^{n_K} \omega_m \sum_{\beta=1}^{m} \lambda_{\beta-1} + \delta_K + \delta_{K+2} - 2\delta_{K+1} \tag{8.4.8}$$

The quantities

$$S_K = \sum_{i=1}^{n_K} \lambda_i \sum_{\gamma=1}^{i} \omega_\gamma \tag{8.4.9}$$

and

$$T_K = \sum_{j=1}^{n_K} \omega_j \sum_{l=1}^{j} \lambda_{l-1} \tag{8.4.10}$$

shall be called the respective fore and aft scatter moments of cell K, They are statistical variables that fluctuate from cell to cell. Each has an expectation value of zero.

One may notice that:

$$S_K + T_K = t\sum_{i=1}^{n_K} \omega_i = t(\phi_{K+1} - \phi_K) \equiv 2\psi_K \tag{8.4.11}$$

is t times the angle turned through in the Kth cell. We define another variable, χ_K, as follows:

$$2\chi_K \equiv S_K - T_K \tag{8.4.12}$$

The mean value $\langle S_K^2 \rangle$ of S_K^2 is equal to the mean value $\langle T_K^2 \rangle$ of T_K^2. Therefore the mean value

$$\langle \chi_K \psi_K \rangle = \tfrac{1}{4}[\langle S_K^2 \rangle - \langle T_K^2 \rangle] = 0$$

The following, then, are rather obvious:

$$\langle \chi_K \delta_K \rangle = \langle \chi_K \delta_l \rangle = \langle \psi_K \delta_K \rangle = \langle \psi_K \delta_l \rangle = 0$$

These are mean values for very large samples or *expectation* values.

Also, for $K \neq l$:

$$\langle \chi_K \psi_l \rangle = \langle \psi_K \psi_l \rangle = \langle \chi_K \chi_l \rangle = 0$$

and

$$\langle \psi_K^2 \rangle = 3\langle \chi_K^2 \rangle = \frac{n_K t^2}{4} \langle \omega^2 \rangle$$

The variables ψ, χ, and δ are therefore independent statistical variables. The average value of n_K is $N\sigma t$, so we have the exact relations:

$$\Delta_t^2 = 8/3\langle \psi^2 \rangle = 8\langle \chi^2 \rangle = (2/3)\, N\sigma t^3 \langle \omega^2 \rangle = 2/3 t^2 \langle \phi^2 \rangle = (1/3)\theta_s^2 t^3$$

Here Δ_t^2 is the mean square noise-corrected second difference derived from cell t without cut off.

It is proved by induction that the rth difference, D_K^r, constructed on y_K is:

$$\begin{aligned} D_K^r = &\sum_{\alpha=1}^{r} \frac{(-1)^{r-\alpha}(r-2)!\,(2\alpha - r - 1)}{(r-\alpha)!\,(\alpha-1)!} \psi_{K+\alpha-1} \\ &+ \sum_{\alpha=1}^{r} \frac{(-1)^{r-\alpha}(r-1)!}{(r-\alpha)!\,(\alpha-1)!} \chi_{K+\alpha-1} \\ &+ \sum_{\alpha=0}^{r} \frac{(-1)^{r-\alpha} r!}{(r-\alpha)!\,\alpha!} \delta_{K+\alpha} \qquad \text{for } r \geqslant 2. \end{aligned} \tag{8.4.13}$$

Differences, D_K^r of all orders are homogeneous linear combinations of the independent quantities ψ, χ, and δ. Difference products are homogeneous quadratic expressions in these quantities. In the mean values, cross products do not occur. In general:

$$\langle D_K^r D_{K+l}^r \rangle = \left\{ \frac{\Delta_t^2 (-1)^l [(r-2)!]^2}{8} \right\} \times \left[\sum_{\alpha=1}^{r-l} \frac{(r-1)^2 + 3(2\alpha - r - 1)(2\alpha + 2l - r - 1)}{(r-\alpha)!\,(\alpha-1)!\,(r-\alpha-l)!\,(\alpha+l-1)!} \right] + \langle \delta^2 \rangle (-1)^l [r!]^2 \sum_{\beta=0}^{r-l} \frac{1}{(r-\beta-l)!\,(\beta+l)!\,(r-\beta)!\,\beta!} \tag{8.4.14}$$

As particular examples,

$$\langle D_K''^2 \rangle = \Delta_t^2 + 6\langle \delta^2 \rangle$$

$$\langle D_K'' D_{K+1}'' \rangle = \frac{\Delta_t^2}{4} - 4\langle \delta^2 \rangle$$

$$\langle D_K'' D_{K+2}'' \rangle = \langle \delta^2 \rangle$$

$$\langle D_K'''^2 \rangle = 3/2\Delta_t^2 + 20\langle \delta^2 \rangle$$

etc.

The relations in Eq. (8.4.14) are exact if one measures tracks for which the small-angle approximation is valid. In particular, the relations do not depend for their validity on assumptions regarding the scattering distribution law. Unless it makes for much greater convenience to do so, and accuracy can be sacrificed, it is better not to assume a Gaussian distribution. For a scattering variable X, a Gaussian distribution would imply $\langle\,|\,X\,|\,\rangle = (2/\pi)^{1/2}\langle X^2 \rangle^{1/2}$.

In later applications of the scattering formulas there may arise some confusion regarding symbols unless they are summarized here. By D_K'' we mean the algebraic value (calculated on ordinate y_K) of $y_K - 2y_{K+1} + y_{K+2}$. By $\langle D''^2 \rangle$ we mean the value of the quantity $D_K''^2$ averaged over many successive cells. By $D_K'' D_{K+j}''$ we mean the product of the algebraic values D_K'' and D_{K+j}'' of measurements calculated on y_K and y_{K+j}. By Δ_K^2 we mean the value $D_K''^2$ corrected for noise. By Δ_t^2 we mean Δ_K^2 averaged over many cells of length t. By D_K we mean $|\,D_K''\,|$ corrected for noise. By D_t we mean the average value of D_K from many cells. In the Gaussian approximation $\Delta_t^2 = (\pi/2)D_t^2$. The quantity $D_{K,m}''$ is the algebraic

second difference $y_K - 2y_{K+m} + 2y_{K+2m}$ calculated on ordinate K with cells each consisting of the sum of m unit cells. By $\langle \mid D'' \mid_m \rangle$ is meant the mean value of the absolute second difference for a cell of m times the unit cell. The unit cell is conventionally 100 μ in length. The noise-corrected sagitta D for such a cell carries no subscript. Parallel notation is extended to the rth differences D^r_K.

8.5 Correlation between Track Direction and Track Displacement

When a charged particle, originally directed along the x axis, has penetrated a scattering medium a distance t, it will be found displaced a distance y along the y axis. Also, it will be directed along a line making an angle ϕ in the x, y plane with its original direction. The displacement, y, and the angle, ϕ, are random but correlated variables. Fermi (R 52) solved the problem of their correlation with certain simplifying assumptions. These are: (*a*) the energy loss in the absorber is neglected; (*b*) the angle ϕ is small; (*c*) the effects of particle polarization are not considered; (*d*) both the angle ϕ and the displacement, y, are the resultants of many small scattering events.

Following the general method of Fermi let $F(t, y, \phi)dyd\phi$ be the probability that at the depth of penetration, t, the particle will be found in the (y, ϕ) interval $dyd\phi$. Also, let $\rho(\omega, dt)d\omega$ be the probability that in moving a distance dt that the particle will be deflected through an angle between ω and $\omega + d\omega$.
Then:

$$\rho(\omega, dt) = \rho(-\omega, dt)$$

$$\int_{-\infty}^{\infty} \rho \, d\omega = 1$$

$$\int_{-\infty}^{\infty} \omega^2 \rho(\omega, dt) \, d\omega = \langle \phi^2 \rangle_{dt} = \frac{K_0^2 z^2 dt}{2p^2\beta^2}$$

These limits of integration mean that the integral is to be made over all angles of deflection. K_0 is a scattering "constant" for the unprojected scattering angles, so the factor 2 appears in the denominator. Now the displacement probability distribution varies with t as follows: $F(t + dt, y, \phi) = F(t, y - \phi dt, \phi) = F(t, y, \phi) - (\partial F/\partial y)\phi dt + \cdots$.

The angular probability distribution is also altered in traversing the path interval dt. From the definition of ρ: $F(t + dt, y, \phi) = \int_{-\infty}^{\infty} F(t, y, \phi - \omega) \, \rho(\omega, dt) \, d\omega$.

In order to carry out the integration, $F(t, y, \phi - \omega)$ may be expanded

in powers of ω, since ρ becomes very small for large values of ω. On dropping terms higher than the second degree in ω this gives:

$$F(t, y, \phi - \omega) = F(t, y, \phi) - \omega \frac{\partial F}{\partial \phi} + \frac{1}{2} \frac{\partial^2 F}{\partial \phi^2} \omega^2$$

Therefore

$$F(t + dt, y, \phi) = F(t, y, \phi) + \frac{1}{4} \frac{\partial^2 F}{\partial \phi^2} \cdot \frac{K_0^2 z^2}{p^2 \beta^2} dt \tag{8.5.1}$$

The total change of F in the layer dt is then

$$\left(-\phi \frac{\partial F}{\partial y} + \frac{1}{4} \frac{K_0^2 z^2}{p^2 \beta^2} \frac{\partial^2 F}{\partial \phi^2} \right) dt$$

so that

$$\frac{\partial F}{\partial t} = -\phi \frac{\partial F}{\partial y} + \frac{\theta_s^2}{4} \frac{\partial^2 F}{\partial \phi^2} \tag{8.5.2}$$

We have defined $1/\theta_s = (p\beta)/(zK_0)$. Fermi found the solution of Eq. (8.5.2) corresponding to a single incident particle to be:

$$F(t, y, \phi) = \frac{2(3)^{1/2}}{\pi} \frac{1}{\theta_s^2 t^2} \exp \left[-\frac{4}{\theta_s^2} \left(\frac{\phi^2}{t} - \frac{3y\phi}{t^2} + \frac{3y^2}{t^3} \right) \right] \tag{8.5.3}$$

This solution was obtained in a different way by Molière (M 55). On integrating it over y, one obtains the angular distribution $G(t, \phi)$:

$$G(t, \phi) = \frac{1}{(\pi)^{1/2}} \frac{1}{\theta_s t^{1/2}} \exp \left[-\frac{\phi^2}{\theta_s^2 t} \right] \tag{8.5.4}$$

If, instead, we integrate over ϕ we obtain the distribution $H(t, y)$ in y:

$$H(t, y) = \frac{(3)^{1/2}}{(\pi)^{1/2}} \frac{1}{\theta_s t^{3/2}} \exp \left[-\frac{3y^2}{\theta_s^2 t^3} \right] \tag{8.5.5}$$

The circumstance that Eqs. (8.5.4) and (8.5.5) are Gaussian in ϕ and y is, of course, a result of the simplifications introduced by dropping terms of higher degree than dt and ω^2. This sometimes may be quite unjustified.

Eq. (8.5.3), however, elegantly describes not only the angular distribution for each particular displacement, but also the displacement distribution for any given scattering angle, subject to the conditions (*a*), (*b*), (*c*), and (*d*).

This solution is valid for noninteracting particles of high velocity in a thick absorber. At low velocities the assumption of no energy loss along the track is not justified. Eyges (E 48) has found a solution of Eq. (8.5.2) when θ_s is a function of t.* In Section 8.11 we calculate $\langle y^2 \rangle$ and $\langle \phi^2 \rangle$ in a simpler way including the energy-loss effect.

8.6 Scattering Caused by Electrons

The main effect of the electronic charge density in the atom on the scattering of an energetic charged particle is that of nuclear screening. The electron cloud is not a structureless fluid, however, and effects of the finite mass and concentrated charge of the electron are also manifested in the scattering.

In a close collision with an electron at rest, a heavy particle of momentum p will suffer a small deflection θ_e, which is given by:

$$\cos \theta_e \approx 1 - \frac{mw}{p^2}$$

In this equation w is the energy transfer to the electron. When w exceeds a few electron kilovolts the electron is called a delta ray.

As long as θ_e is small one may also write:

$$\theta_e^2 \approx \frac{2mw}{p^2} \tag{8.6.1}$$

The cross section for transfer of energy between w and $w + dw$ to an electron by a particle of charge ze is given by Eq. (9.1.1).

In a medium where there are n electrons per unit volume, the mean square value, $\langle \theta^2 \rangle_e$, of the deflection produced by electrons is found using Eq. (9.1.1). It is

$$\langle \theta^2 \rangle_e = n \int \theta_e^2 \frac{d\sigma}{dw}\, dw \text{ per cm}$$

or

$$\langle \theta^2 \rangle_e = \frac{2nm}{p^2} \int w \left(\frac{d\sigma}{dw} \right) dw \text{ per cm} \tag{8.6.2}$$

Aside from a factor (m/p^2) this is the same as the expression in Eq. (9.2.1) which gives the energy loss in unit path of the heavy particle. Therefore,

$$\langle \theta^2 \rangle_e \approx 2\langle \phi_e^2 \rangle = m\mathcal{I}/p^2 \tag{8.6.3}$$

* In Eyges' Eq. (15) there is an error. The exponent should not contain the factor t that appears in the denominator.

The mean square angle of nuclear scattering of an atom is proportional to the square of its atomic number while the electronic scattering effect increases only proportional to the atomic number. Therefore, the electronic scattering is important in hydrogen, but of decreasing importance as the atomic number increases.

Williams (W 40) has approximated the specific scattering effect of electrons merely by writing $Z(Z+1)$ for Z^2 in the atomic scattering formulas. From Section 8.7, the mean-square projected scattering angle is given by

$$\langle \phi^2 \rangle = \frac{3\pi^3 K^2 z^2 t}{4(18)^2 p^2 \beta^2} \tag{8.6.4}$$

The ratio $\langle \phi^2 \rangle_e / \langle \phi^2 \rangle$ in emulsion, therefore, is about 0.01 for a relativistic particle. The factor $\langle 1 + (1/Z) \rangle$ is seen somewhat to overestimate the scattering by the electrons in emulsion. Of course, the effect estimated by Eq. (8.6.4) is solely of the *inelastic* scattering. The adiabatic interactions produce the nuclear screening, and Eq. (8.2.1) would seem to include their scattering effect.

8.7 The Scattering Factor

Thus far we have been concerned with a description of the multiple scattering that did not require explicit evaluation of the elementary differential scattering cross section. Now we must determine, as accurately as possible, the deflections ω in atomic fields, and calculate the resultant of plurality of such deviations.

8.7.1 Multiple Scattering Distribution Function

At a depth of penetration t, let the fraction of projected angles, ϕ, in the interval $d\phi$ be $f(\phi, t)\, d\phi$. The angle ϕ may be the resultant of many individual deflections. In the scattering process, let the fraction of projected elementary deflections that lie between ω and $\omega + d\omega$ be $\rho(\omega)\, d\omega$. Then we can construct the following equation.

$$\frac{\partial f(\phi, t)}{\partial t} = N\sigma \int_{-\infty}^{\infty} [f(\phi - \omega, t) - f(\phi, t)]\, \rho(\omega)\, d\omega \tag{8.7.1}$$

Where N is the number of scattering atoms per unit volume and σ is the total scattering cross section of an atom. Following the method of Snyder and Scott (SS 49), we find the solution of Eq.(8.7.1) in the form:

$$f(\phi, t) = \frac{\exp(-N\sigma t)}{\pi} \int_{s=-\infty}^{\infty} \cos(\phi s) \exp\left[N\sigma t \int_{-\infty}^{\infty} \rho(\omega) \cos(s\omega)\, d\omega\right] ds \tag{8.7.2}$$

The connections between the moments of the ω-distribution and the ϕ-distribution are of considerable practical importance. Since

$$\phi = \sum_1^n \omega_i$$

where n is the number $N\sigma t$ of deflections in path t, $\langle \phi^r \rangle = \langle (\Sigma \omega_i)^r \rangle$. All the moments of the multiple scattering distribution, therefore, can be derived from the elementary scattering distribution. Thus

$$\langle \phi^2 \rangle = N\sigma t \langle \omega^2 \rangle$$
$$\langle \phi^4 \rangle = N\sigma t \langle \omega^4 \rangle + 3(N\sigma t \langle \omega^2 \rangle)^2$$
$$\langle \phi^6 \rangle = N\sigma t (\omega^6 \rangle + 15(N\sigma t)^2 \langle \omega^2 \rangle \langle \omega^4 \rangle + 15(N\sigma t \langle \omega^2 \rangle)^3$$
etc.

For unpolarized particles, the odd moments vanish, and in general:

$$\frac{d\langle \phi^{2m} \rangle}{dt} = N\sigma \sum_{j=1}^{m} \frac{(2m)! \langle \omega^{2j} \rangle \langle \phi^{2(m-j)} \rangle}{[2(m-j)]! (2j)!} \tag{8.7.3}$$

Now one can invert the problem and ask for the moments of the elementary scattering distribution, having measured only the *multiple* scattering distribution. He finds:

$$\langle \omega^2 \rangle = \langle \phi^2 \rangle / (N\sigma t)$$
$$\langle \omega^4 \rangle = (\langle \phi^4 \rangle - 3\langle \phi^2 \rangle^2)/(N\sigma t) \tag{8.7.4}$$
$$\langle \omega^6 \rangle = [\langle \phi^6 \rangle - 15\langle \phi^4 \rangle \langle \phi^2 \rangle + 30\langle \phi^2 \rangle^3]/(N\sigma t)$$
etc.

It should be noticed that the value of $N\sigma t$ and the moments of the elementary scattering distribution depend very much on the small-angle distribution given by the screening calculation. The product $N\sigma t \langle \omega^{2m} \rangle$, however, is not sensitive to this calculation if the theory has been carried through consistently. Thus, for example, if Molière's theory of screening is applied, it is essential that his Ω [Eq. (8.7.13)] be adopted as the estimate of $N\sigma t$.

8.7.2 Introduction of the Scattering Factor

For small angles, Eq. (8.1.4) for the probability of scattering into $d\omega$ in unit emulsion path becomes

$$p(\omega)\, d\omega \approx \frac{2.35z^2}{p^2\beta^2} \frac{d\omega}{\omega^3}$$

As discussed in Section 8.2, electron screening and the finite size of the nucleus affect this cross section by a factor $Q = Q(\beta, \omega)$. The exact formula for small angles is:

$$\rho(\omega)\, d\omega = \frac{2.35 z^2 Q}{p^2\beta^2} \frac{d\omega}{\omega^3} \tag{8.7.5}$$

and

$$\langle \phi^2 \rangle = \frac{2.35 z^2 t}{p^2\beta^2} \int_{-\infty}^{\infty} Q \frac{d\omega}{\omega}$$

Now

$$\langle \alpha^2 \rangle = (2/3)\langle \phi^2 \rangle = \frac{1.567 t z^2}{p^2\beta^2} \int_{-\infty}^{\infty} Q \frac{d\omega}{\omega}$$

In the Gaussian approximation $\langle \alpha^2 \rangle = \pi/2(\bar{\alpha})^2$. So, when expressed in degrees:

$$\bar{\alpha} = 5.73 \left[\int_{-\infty}^{\infty} Q \frac{d\omega}{\omega}\right]^{1/2} \frac{z}{p\beta} \left(\frac{t}{100}\right)^{1/2} \tag{8.7.6}$$

In Eq. (8.7.6), t is to be expressed in microns. The quantity

$$K = 5.73 \left[\int_{-\infty}^{\infty} Q \frac{d\omega}{\omega}\right]^{1/2}$$

is sometimes called the scattering "constant." It is better described as the scattering "factor." Because Q varies slowly with velocity, and the Gaussian approximation has been made, K is not strictly a constant. It varies with particle velocity and cell length in a particular scattering material such as emulsion. Its numerical value depends somewhat on the theory used in its calculation, and the cut-off procedure applied (see below).

We shall make some comparisons later of theories, and also of theory with the observations.

The absolute mean scattering angle, $\bar{\alpha}$, between successive chords conventionally is written:

$$\bar{\alpha} = \frac{Kz}{p\beta} \left(\frac{t}{100}\right)^{1/2} \tag{8.7.7}$$

Here $\bar{\alpha}$ is measured in degrees, K in Mev/c, ze is the charge on the moving particle, and t is in microns. Measurements are seldom reduced to an angle in current practice, however. If the mean absolute second difference corrected for noise and measured in microns is D_t then

$$D_t = \frac{\langle \bar{\alpha} \rangle\, t}{57.3}, \quad \text{or} \quad D_t = \frac{K z t^{3/2}}{573 p\beta}$$

Consequently, $p\beta/z = (Kt^{3/2})/(573D_t)$. When, as recommended below, a cut off has been applied, one uses the formula

$$\frac{p\beta}{z} = \frac{K_c t^{3/2}}{573 D_{ct}} \tag{8.7.8}$$

8.7.3 Cut Off of Large Deflections

As long as the scattering is by the nuclear electric field alone, the behavior of all elementary charged particles is the same. Nuclei are finite in size, however, and in their interaction behavior various particles differ profoundly. Multiple scattering measurements can be carried out in such a way as to eliminate the effects of strong interactions as well as the occasional large-angle Coulomb deflections. To accomplish this it is usual to exclude large angles according to some prescription. In the Fowler method of measurement, it is conventional to eliminate second differences exceeding four times the resultant mean second difference.

Suppose that the small-angle scattering is described by a Gaussian of variance σ^2. Then the mean value $\langle\,|\,x\,|\,\rangle$ of the variable with cut off is

$$\langle|\,x\,|\rangle = \frac{\int_0^{4\langle|x|\rangle} x \exp\left(-x^2/2\sigma^2\right) dx}{\int_0^{4\langle|x|\rangle} \exp\left(-x^2/2\sigma^2\right) dx} \tag{8.7.9}$$

Solving this equation for $\langle\,|\,x\,|\,\rangle$, we find $\langle\,|\,x\,|\,\rangle = 0.993(2/\pi)^{1/2}\,\sigma$. A Gaussian without cut off gives $(2/\pi)^{1/2}\,\sigma$, so that usually one need not distinguish between a cut off Gaussian and a Gaussian, whereas a non-Gaussian tail may be largely eliminated.

Another cut-off method has been devised by Lipkin, Rosendorff, and Yekutielli (LRY 55) which is specifically designed to minimize fluctuations caused by the tail of the Molière distribution (see below).

A correctly applied cut off procedure eliminates occasional large fluctuations in the measurements, and also insures that the measured scattering is the response of the particle to electric forces alone. The method in which large deviations are replaced by the maximum permitted deviation is a possible alternative, but it is somewhat erroneous in principle. For a given $p\beta/z$, an effect of strong interactions will still be present in the measured mean scattering angle because the *number* of large deviations depends on the nature of the interaction. In practice this is rather a fine point, however, because the mean free path for nuclear interaction is great.

On the other hand, sometimes something about the nature of a particle producing a long track can be determined by an analysis of

the large angular deviations. The smallest deflection consistently measureable with a field of 200 μ and a magnification of 600 is perhaps 0.5° (G 50). An analysis of antiproton tracks was carried out in this way by Goldhaber and Sandweiss (GS 58). They recorded elastic scattering events of a projected angle greater than 2°. They found for antiprotons of energy 50-200 Mev that the scattering is as if each nucleus had an effective radius $r_0 A^{1/3}$ with $r_0 = 1.64 \times 10^{-13}$ cm inside of which all partial waves of the antiproton were absorbed. This radius corresponds to the measured annihilation cross section of emulsion nuclei.

8.7.4 Molière's Angular Distribution

Currently, the best-known theory of multiple scattering is that of Molière (M 48, M 55) although the writings of Wentzel (W 22), Bothe (B 29), Williams (W 39, W 40), Olbert (O 52), Goudsmit and Saunderson (GS 40), Snyder and Scott (SS 49), Lewis (L 50.2), Scott (S 52), and others have made important contributions to the thinking on this subject. Even the Molière theory adopts an approximation for the atom model of Thomas-Fermi in calculating the elementary scattering distribution. Moreover, Molière makes no allowance for the finite size of the nucleus. The angular distribution at large angles of deflection is derived by considering only the Coulomb force of a point nucleus. Finally, Molière's mathematical procedures have been questioned (NSW 59). Nevertheless, considerable empirical evidence confirms the general correctness of his distribution except in the tail.

For small scattering angles Molière's distribution becomes the same as that derived with the Born approximation and for large angles the same as the Rutherford Law. The intermediate angles are bridged by the WKB method.

For calculating the multiple scattering it is necessary to have an accurate elementary scattering law, and also to evaluate correctly the effective number of scattering events contributing to the resultant deflection.

Let σ be the "total" scattering cross section of an atom. Then the average number of collisions in path t is $N\sigma t$, but most of these collisions contribute virtually nothing to the multiple scattering. They consist of small deflections experienced in traversing the interpenetrating outer envelopes of atoms. In this region the nuclei are heavily screened and calculations are difficult. A screening angle, χ_a, which for the purposes of multiple scattering calculations may sufficiently describe the elementary scattering distribution was introduced by Molière (M 47). He symbolized by $q(\chi)$ the ratio of the atomic scattering cross section for space angle χ

to the Rutherford cross section. Then $q(\chi)$ was expressed approximately by the simple formula

$$q(\chi) = \frac{\chi^4}{(\chi^2 + \chi^2{}_a)^2} \tag{8.7.10}$$

In this formula χ_a, the screening angle is chosen so that with the function of Eq. (8.7.10) the same mean absolute scattering angle is predicted as he finds from detailed calculations with an approximation to the Thomas-Fermi atom. The single angle, χ_a, determines the scattering. It is calculated from

$$\chi_a = \frac{1.063\hbar}{ap\beta}\sqrt{\beta^2 + \left(\frac{zZ}{75}\right)^2} \tag{8.7.11}$$

where a is the radius of the Thomas-Fermi atom ($0.885a_0Z^{-1/3}$), and a_0 is the Bohr radius, $\hbar^2/me^2$. An angular unit χ_c is defined by

$$\chi_c^2 = \frac{4\pi Nte^4Z(Z+1)\,z^2}{(p\beta)^2} \tag{8.7.12}$$

The total probability is unity that in path t the particle will scatter through an angle greater than χ_c.

The *effective* number of collisions in path t (in centimeters) is

$$\Omega = \chi_c^2/\chi_a^2, \quad \text{or} \quad \Omega = \frac{1.47 \times 10^{-20}Ntz^2Z^{1/3}(Z+1)}{\beta^2 + (zZ/75)^2} \tag{8.7.13}$$

A quantity B, related to Ω enters the theory frequently. It is found from

$$\ln \Omega = 0.115 + B - \ln B \tag{8.7.14}$$

A more convenient approximation for B has been given by Scott (S 52). It is

$$B = 1.153 + 2.583 \log_{10} \Omega \tag{8.7.15}$$

for $\Omega > 100$.

Molière employed a transport equation specialized to his elementary scattering law. It is otherwise equivalent to Eq. (8.7.1). By a Bessel-Fourier integral transformation and other rather formal analytical

procedures he develops the solution for the projected multiple scattering angle ϕ in inverse powers of B as follows:

$$f(\phi, t)\, d\phi = \frac{d\phi}{\chi_c (B)^{1/2}} \times \left\{ \frac{2}{(\pi)^{1/2}} \exp\left(-\frac{\phi^2}{\chi_c^2 B}\right) + \frac{1}{B} f^{(1)}\left[\frac{\phi}{\chi_c (B)^{1/2}}\right] + \frac{1}{B^2} f^{(2)}\left[\frac{\phi}{\chi_c (B)^{1/2}}\right] + \cdots \right\} \tag{8.7.16}$$

The function $f^{(1)}$ and $f^{(2)}$ have been tabulated in Molière's (M 48) paper.

8.7.5 Numerical Evaluation of Scattering Factors for Emulsion

Although Eq. (8.7.16) is relatively simple for a pure element, it becomes rather cumbersome if one considers all the elements making up emulsion. Some approximation is necessary. Fortunately the dependence of B on Z is slight so that the method of averaging over the emulsion elements is of little importance.

To evaluate the scattering factor, Scott (S 52) first compared the theory of Molière (M 48) with that of Snyder and Scott (SS 49). The theories were found to be mathematically equivalent if the single scattering formula and screening angle of Molière were introduced into Snyder and Scott's theory. Scott then calculated scattering factors with various cut-off assumptions. Some of his results are given in Table 8.7.1. The absolute mean angle without cut off given by Molière's theory is inapplicable because he assumed a point nucleus, and the "no cut off" scattering factors are included here only for comparison. The meanings of the various symbols we use are as follows:

(a) K, scattering factor for mean absolute projected angle, $\bar{a}$, between chords without cut off;

(b) K_c, scattering factor for mean absolute projected angle, $\bar{a}_c$, between chords with cut off at four times the cut off mean;

(c) K_e, scattering factor for a mean projected angle, $\bar{a}_e$, between chords corresponding to an ordinate $1/e$ times the maximum ordinate;

(d) K', the scattering factor for the mean absolute projected angle, $\langle\, |\, \phi\, |\, \rangle$, between tangents without cut off.

(e) K'_c, the scattering factor for the mean absolute projected angle, $\langle\, |\, \phi\, |\, \rangle_c$, measured between tangents and cut off at $4\langle\, |\, \phi\, |\, \rangle_c$; and

(f) K'_e, the scattering factor for a mean projected angle, ϕ_e, between tangents corresponding to an ordinate lower by a factor e than the ordinate at $\phi = 0$. The scattering factor in each case can be written

$$K^2 = 675[a + b \log_{10} \Omega] \tag{8.7.17}$$

Table 8.7.1 gives the values of a and b for each scattering factor.

TABLE 8.7.1
COEFFICIENTS a AND b FOR CALCULATING SCATTERING FACTORS

Coef.	K	K_e	K_e	K'	K_c'	K_e'
a	0.299	0.090	−0.105	1.044	0.418	0.253
b	0.269	0.272	0.879	0.809	0.818	2.636

Scattering factors for cut off and replacement by the cut off value are not quoted for the reason given above.

The part of the Molière formula that applies generally is the Gaussian term. Each elementary particle has its own characteristic large-angle scattering behavior, and in a prescription for measuring $p\beta/z$ one must eliminate particle idiosyncracies. In this volume we have chosen to limit the treatment to the conventional cut off at four times the resultant mean. There is only a slight effect of the Molière functions $f^{(1)}$ and $f^{(2)}$ at small angles, and for simplicity, one could disregard them. This is justified especially because the corrections in this angular range differ from those of Molière when more refined atom models than his are employed.

Mean square scattering angles, because of the small angle approximation and point nucleus assumed, are undefined in the Molière theory.

The coefficient 675 in Eq. (8.7.17) has been adjusted somewhat from the value given by Scott because we use the more exact emulsion composition of Table 3.5.1. From this we calculate $\Sigma N_i Z_i^2 = 3.61 \times 10^{25}$ per ml. In addition we correct for scattering by electrons. The effect of the Molière factor $[\beta^2 + (zZ/75)^2]$ is approximately $[\beta^2 + 0.30z^2]$ when summed over the emulsion elements. Allowance for the velocity and particle-charge dependence of the scattering factor, accordingly, can be made if we define an equivalent cell t_1, such that

$$t = \left(0.23 + 0.77\frac{\beta^2}{z^2}\right) t_1 \tag{8.7.18}$$

This formula gives the cell length t for $\beta/z \neq 1$ that has the same scattering factor as a cell of length t_1 with $\beta = 1$.

The scattering factor K_c for $\bar{a}_c$ in degrees, $p\beta$ in Mev/c, t_1 in microns, and $\beta = 1$, as calculated from Eq. (8.7.17), is given in Table 8.7.2.

TABLE 8.7.2
THE SCATTERING FACTOR K_c FOR $\beta = 1$

t_1	$10\ \mu$	$10^2\ \mu$	$10^3\ \mu$	$10^4\ \mu$	$10^5\ \mu$
K_c	19.3	23.6	27.2	30.4	33.3

We also find from Eq. (8.7.13) that

$$\Omega = 5t_1 \tag{8.7.19}$$

and from Eq. (8.7.15)

$$B = 2.45 + 2.58 \log_{10} t_1 \tag{8.7.20}$$

when t_1 is in microns.

8.7.6 Some Studies of the Scattering Factor

Voyvodic and Pickup (VP 52) carried out a useful study of the scattering factor in which they compared the predictions of the various scattering theories and studied the effect of cutting off the large scattering angles. They also compared the predictions with measurements in emulsion. They improved the theory of Williams (W 39) by making the transition between the Born approximation and Rutherford regions through the Molière factor $(\beta^2/z^2 + 0.30)$, as in Eq. (8.7.13). With this adjustment they obtained essentially the same results whether they employed the theories of Williams, Snyder and Scott, or Molière, but because of its greater simplicity the Williams theory was preferred for calculations. On the basis of Williams theory, the mean absolute angle $\bar{\alpha}_c$ after cut off at $4\bar{\alpha}_c$ is given by

$$\bar{\alpha}_c = \frac{\bar{\alpha} - \pi/(4\bar{\alpha})}{1 - \pi/(32\bar{\alpha}^2)} \tag{8.7.21}$$

The adjusted Williams formula for the scattering factor without cut off including the electron-scattering effect is

$$K = 12.1 \left\{1 + 0.837 \left[\left\{\left(\frac{\beta}{z}\right)^2 + 0.30\right\}^{-1} \log_{10}(0.94t)\right]^{1/2}\right\}$$

The units are degrees, Mev/c, and microns.

The scattering factors calculated by Voyvodic and Pickup were found to be generally in good agreement with the measurements they made on fast electrons, and with the published observations (C 51, BLS 51, G-R 51,

MOR 51) on the scattering of electrons and protons in emulsion. Thus, for example, K_c for electron pairs of 16.7 Mev was calculated to be 22.1 whereas they measured 21.2 ± 0.7 using an average cell of 45 μ. The energies of the electron pairs were determined by scattering 700 μ of track from each member of the pair. The energy of the pair was found to be measured with a statistical uncertainty of 10%. Electron-pair energies have been measured by this method in a number of other studies. For example, Heckman, Giles, and Barkas (HGB 54), and Giles (G 53), observed the π°-γ-ray spectrum emitted at 90° from a beryllium target when it was bombarded by 330 Mev protons. On measuring the scattering of pairs produced in 400 μ emulsion by monoenergetic 6.14 Mev photons, it was found that the energy resolution was 1.37 Mev. (This is the standard deviation of the apparent energy distribution, and the energy was correctly given by the scattering.)

On tracks of 6.2 Bev protons Biswas, Prasad, and Mitra (BPM 57) measured a scattering factor about 10% higher than that given by Voyvodic and Pickup when cells of 1, 2, and 3 mm were employed.

The scattering factor for cells longer than a few millimeters is not known to be reliable. Recent work with very long cells on tracks of high-energy pions and muons has led Hossain *et al.* (HVWE 61) to recommend a scattering factor of $27.6 \pm 0.6°$ Mev/c for cell-size range from 1 mm to 3 cm.

Scattering measurements have also been made on the tracks of heavy nuclei. Dainton, Fowler, and Kent (DFK 51) obtained consistent results using a value of $26° \times$ Mev/c for the scattering factor of multiply charged particles in cosmic rays.

Backus, Lord, and Schein (BLS 52) found scattering factors K_c, of 24.8 ± 1.4 for a 250 μ cell, and 26.2 ± 2.2 for a 500 μ cell when they scattered tracks of carbon nuclei, the energies of which varied from 10 to 1000 Mev. Their measurements on protons and pions checked well with theory.

In the Lawrence Radiation Laboratory W. G. Simon has investigated the multiple scattering distributions of A^{40} and O^{16} ions in gold, aluminum and zapon. The agreement with Molière is generally good.

8.8 Measurement Procedure

The scattering of a particle in emulsion is independent of the emulsion sensitivity, and of its degree of development. If one has a reliable measure of the scattering, this can be used to determine the product, $p\beta/z$, of the particle magnetic rigidity and its velocity.

8.8.1 Track Tangent Method

A measurable quantity of this sort is the average absolute change of the projected particle direction, $\langle | \phi | \rangle = \langle | \phi_{K+1} - \phi_K | \rangle$ in path length t. The track direction is observed at many points spaced by a distance t, and the absolute angular changes in direction are averaged. Early workers (L 48, GKMR 48, DLM 49) projected a real image of the track and measured the scattering angles on the enlarged projection.

A protractor or goniometer used by Goldschmidt-Clermont (G 50) consists of a moving arm fixed to the eyepiece of the microscope which can be adjusted by means of a tangential screw. The moving arm bears either a good vernier or a reading microscope so that a fraction of a minute of angle can be read. The eyepiece is fitted with a straight-line reticle which is placed tangent to the track at points separated by the cell length t. The stage motion was found to be parallel to a straight line to 2 min for 3- and 7-cm displacements (G 50). The inaccuracy with which the true tangent to the trajectory is determined with the reticle is the "noise." This is reduced by making several reticle settings on the track at each point of measurement. The lower limit of the total noise is about 2 min of angle for 400-600 μ emulsions.

Rankin (R 54) by a rather simple optical-lever principle was able to construct a goniometer that enabled him easily to measure ϕ to 0.05° by means of a scale appearing in the microscope field of view. This made it unnecessary to take the eye from the track during measurement. Measurements were made simply and rapidly.

Cosyns (C 51) constructed a split-image microscope so that one image of a track crossing the center of the field remained stationary and another, of opposite reflection symmetry, rotated when the system of reflecting prisms was caused to rotate. At an arbitrary position of the prism system the two track images crossed in the field. At a critical position the two images were superimposed. When the track was straight, the two images of a grain would overlap and the contrast would increase appreciably. When the images were most exactly superimposed a scale in the field of view could be illuminated and the angle ϕ_K of the track segment could be read directly.

To fit a tangent to a track locus a finite segment of track must be considered. This produces a smoothing in the angular changes $\phi_K - \phi_{K-1}$. Empirically this seems to reduce the scattering effect by about 4%.

8.8.2 Coordinate Method

When only a small length of track is available for measurement, or when the particle is strongly scattered, it may sometimes still be useful to

measure the angle between tangents, but this method of measurement has now been generally superseded by the coordinate method of Fowler (F 50.1). When the mean scattering angle is small the coordinate method is especially preferred.

"Fowler's method" refers to the following general procedure:

The track is aligned approximately with the direction of microscope stage motion, which is taken to be the abscissa, x. It is advisable to align the track well enough so that, if possible, over the interval of measurement, it will remain within the microscope field without changing the y coordinate of the stage.

One selects a length, t, parallel to x as a *cell length*. Often this may be 100 μ or so. The ordinate of the track at an arbitrary $x = 0$ point is recorded as y_0. Then the plate is displaced a distance t along the x axis and the ordinate, y_1, recorded. By successively displacing the plate and at each stop recording the track ordinate, a set of numbers, y_i, is obtained. The measurements are the distances of the track from a straight line that extends generally parallel to the track.

Second differences

$$D''_K = (y_{K+2} - y_{K+1}) - (y_{K+1} - y_K)$$

may then be calculated. The average absolute value $\langle \mid D''_K \mid \rangle$ (Section 8.4) is a measure of the mean angle $\bar{\alpha}$ between successive chords to the track.

When the reading and recording is not done by automatic equipment, usually two people can work together advantageously. The observer operates the microscope controls and reads off the y coordinates. If another person records the data, the observer need not take his eyes from the track or his hands from the controls. Oral transmission of the data to a tape recorder is also possible. Often the human recorder can also calculate the differences and otherwise process the data in the time between readings, and they can alternate tasks.

It is obvious that this method, which obtains minute deviations of the track locus from a straight line, requires special equipment. It is objectionable if irregular stage motion contributes more than a very few hundredths of a micron to the apparent scattering sagitta. In Section 8.12 we discuss the equipment for such measurements.

8.8.3 The Scattering Sagitta

In order to reduce the labor of multiple scattering calculations when they are not carried out by automatic methods, it has been common to to find the absolute second differences, $\mid D''_K \mid$

$$\mid y_K - 2y_{K+1} + y_{K+2} \mid = \mid D''_K \mid \qquad (8.8.1)$$

The mean value of this quantity over many cells and corrected for noise and cell length is the scattering sagitta, D. It is derived for a cell of standard length, normally 100 μ. Using the Gaussian approximation for the noise,

$$D_m^2 = m^3 D^2 + \frac{12}{\pi}\langle\delta^2\rangle_m \tag{8.8.2}$$

is the squared mean absolute second difference for a cell of m times the standard length. "The mean projected scattering angle between chords," $\bar{\alpha}_c$, is given by $\bar{\alpha}_c = (\pi m^{1/2} D_c)/1.8$ when D_c is in microns, $\bar{\alpha}_c$ is expressed in degrees, and D_c is cut off at four times the resultant mean. Scattering factors are quoted for the angle $\bar{\alpha}_c$ in Table 8.7.2.

Sometimes zeros are recorded among absolute second-difference measurements. When this happens it means that the scale of measurement is too coarse. A systematic error is then introduced. When the least distance recorded is a, then to correct this error each zero should be replaced by $a/4$ (BY 54).

The relationships between the angular and coordinate scattering measurements are expressed by Eqs. (8.4.6) and (8.4.8), and by $2/3t^2\langle\phi^2\rangle = 2/3t^2\langle(\phi_K - \phi_{K-1})^2\rangle = \Delta_t^2 \approx \pi/2D_t^2$.

High-energy beams of known momenta from the 25 Bev CERN accelerator have recently subjected the technique and theory of multiple scattering to severe tests. On the whole the method has been found better than expected.

8.9 Track Noise and Its Elimination

The particle path is defined only imperfectly by the track in emulsion because the grains are finite in size and are distributed about the trajectory. The emulsion is also subject to distortion. Additional uncertainties in one's knowledge of the trajectory are introduced during measurement by instrument faults and human error. These various effects are sometimes lumped into the general term "noise." On analysis one finds that they should be subdivided into those that are independent of cell length and others that are not. The former constitute true *noise*. The latter include effects that may be difficult to distinguish from track scattering.

Biswas, Peters, and Rama (BPR 55) classify noise into four types as follows: grain noise, reading noise, stage noise, and temperature noise.

8.9.1 Grain Noise and Reading Noise

The grain noise is affected by the particle velocity and charge as well as by the grain size. It is smaller for emulsion of fine grain and for particles

of low charge. Grains are caused to develop generally along the particle path, but a typical grain center will be displaced from it by a projected distance ϵ. The mean square magnitude $\langle \epsilon^2 \rangle$ of this distance depends on the emulsion grain size, on its sensitivity, and on the particle velocity. The dependence on particle velocity arises because crystals somewhat displaced from the particle path are rendered developable by delta rays. The primary grains consist only of crystals that develop after they are actually traversed by the moving particle. Moreover, when grains develop they may not grow symmetrically about the center of the unprocessed silver halide crystal. The finite grain size and these displacement effects contribute grain noise to the scattering measurement, and also (see Chapter 9) interfere with the measurement of the gap-length distribution in steep tracks. Ekspong (E 54) has evaluated the mean absolute displacement ($\langle | \epsilon | \rangle$ for G.5 emulsion, presumably using the tracks of fast particles. He found $\langle | \epsilon | \rangle = 0.14\ \mu$.

In connection with measurements of π° decay, F. M. Smith (SSB 61) measured the projected value of $\langle \epsilon^2 \rangle^{1/2}$ for tracks in K.5 emulsion. She found it to be only $0.03\ \mu$. In this experiment, however, grains thought to be caused by delta rays were eliminated. The measured grains probably were penetrated by the particles that produced the tracks.

If one attempts to measure the position of a track extending generally along the x axis by averaging the y coordinates of several grain centers, a limitation is encountered. The ordinate of the track cannot be found with a standard deviation of less than $\langle \epsilon^2 \rangle^{1/2}/(gl)^{1/2}$. Here l is the length of the track segment used to establish the y coordinate, and g is the grain density. If a single grain is used, the uncertainty is $\langle \epsilon^2 \rangle^{1/2}$.

The reading error is minimum when track grains are sufficiently close so that the average position of several can be used in locating the true particle trajectory. The error is increased, however, when the grains are so crowded that the track is broadened.

Ekspong (E 54) states that the reproducibility in reading the projected position of a grain is $0.02\ \mu$. (The reader who is unimpressed by this figure should recall that the wavelength of light used in these measurements is about half a micron.)

The individual errors being about $0.023\ \mu$, a total reading error is introduced into the second difference of $0.056\ \mu$ in Ekspong's experience. Other careful measurements are in agreement with these noise estimates. For example, the reading noise and the combined reading and grain noise in Ilford G.5 emulsion was measured on relativistic tracks of particles with various charges by Biswas, Peters, and Rama (BPR 55). For singly charged particles the reading and grain noise together amounted to $0.075\ \mu$. The increasing grain density causes this to fall to $0.06\ \mu$ when

z reaches 3 and the noise passes through a minimum in the interval $z = 3$ to 5. Then, because of the increasing track width, it increases with increasing z, reaching a value of 0.09 μ at $z = 14$. The reading noise remains greater than the grain noise by a factor of about 1.2 for all z in this interval. For a Koristka MS-2 microscope they found, for $z = 4$, that the reading and stage noise together amounted to 0.038 μ and the combined reading, grain and stage noise, was 0.057 μ. Under the same conditions, the combined noise for a singly charged particle was about 0.076 μ. Other observers have found an increase in the noise with increasing cell length. This probably is to be attributed either to stage noise or emulsion distortion. Biswas *et al.* found the noise to be independent of cell length from 10 to 200 μ.

8.9.2 Stage Noise

One of the figures of merit for a scattering microscope is low stage noise. The plate is translated between observations of the track position, and these displacements must be very accurate along a straight line. Biswas, Peters, and Rama state that the stage noise of a Koristka MS-2 microscope increases their total error by less than 0.005 μ for all values of the cell length up to 2000 μ.

A microscope defect that may appear to be stage noise is "focusing noise." As the objective is raised or lowered relative to the stage, either it may not move perpendicularly, or there may be a coupling of the vertical motion with lateral or rotary motions.

The stage noise may depend on the cell length. The total noise of Cooke M-4000 microscopes was found to vary as $t^{0.25}$ by Brisbout *et al.* (B-J 56).

Bøggild and Scharff (BS 54) determined the stage noise by measuring the coordinates $y_0, y_1, y_2, \cdots y_n$ of the track a second time with the plate turned over. The sum of the coordinates then represented the stage noise and the difference describes the shape of the track.

Optical grating lines of good quality were used by Ekspong (E 54) for measuring the noise of the stage motion. In order to see the lines he used phase-contrast optics. Similar measurements on a grating machine scratch were made by Bøggild and Scharff who evaporated aluminum into the scratch and then erased the surface so that the scratch would be visible.

"Straight" lines satisfactory for measuring stage noise can be purchased from optical houses. The line consists of a scratch through a thin metal layer on a glass surface. Flat tracks of very high energy particles in emulsion plates are generally quite satisfactory for over-all noise measurement.

A number of the more elaborate commercial multiple scattering microscopes have as an accessory an optical interferometer.

A very good interferometer is necessary to detect the stage noise of the best instruments. For example, the Zeiss "Kernspurmessmikroskop KSM-1" noise level is stated to be less than 0.02 μ for a 1-mm cell.

Stage noise can also be evaluated by the differential sagitta method (L 50.3), in which one observes y_K and y_{K+1} in a single field of view. Then on shifting the field y_{K+1} is observed a second time along with y_{+K2}.

8.9.3 Temperature Noise

Temperature noise is caused by differential expansions of parts of the microscope so as to cause shifts of the objective lens with respect to the stage. Temperature effects may be reduced by taking a number of precautions. The lamp and other sources of heat should be turned on several hours before measurements are made so that an equilibrium temperature distribution may be attained. In some laboratories, when the room is not thermostated, each microscope is enclosed in a plastic bag into which air at a constant temperature is slowly blown. The bag is not completely air tight around the microscope oculars, etc. The observer himself must avoid introducing body heat effects, and his breath, especially, must be deflected from the microscope. If readings are taken at regular intervals constant temperature drifts will be eliminated on taking second differences. With these precautions temperature effects can be reduced below other unavoidable noise effects.

The measurements of Biswas, Peters, and Rama (BPR 55) give for the temperature noise, ϵ_T, of a Koristka MS-2 microscope

$$\epsilon_T = 3.8 \frac{dT}{dt} \Delta t \, \mu$$

where T is the temperature difference between microscope stage and arm in centigrade degrees, t is the time, and Δt is the mean *variation* in time intervals between successive readings.

8.9.4 Spurious Scattering

The noise effects described above usually are uncorrelated with cell size, and while they introduce an error δ_i in a typical measurement y_i, their effect can be eliminated. Means for doing this will be discussed below. On the other hand, it may be much harder to eliminate effects that increase with cell size and simulate scattering.

The apparent scattering caused by macroscopic distortion of a simple type was evaluated in Section 6.11. This sagitta, D_s, was calculated to be:

$$D_s = \frac{2Kt^2 \sin^2 \theta}{T^2 \tan^2 \delta_0},$$

where t is the projected cell length, θ is the angle of the distortion vector with respect to the x axis, K is the coefficient of the distortion, as defined in Eq. (6.7.5).

A characteristic of this type of distortion is that adjacent second differences tend to have the same sign. Third differences are zero. Even with somewhat more complex types of distortion, an indication of the distortion effects would be larger sagittas calculated from second differences than from third differences. A first approximation correction for simple curvature of the track can be made by subtracting

$$\frac{1}{\nu} \sum_{1}^{\nu} D''_K$$

from all second differences.

Stage curvature or the presence of a strong magnetic field will have the same effect as simple distortion curvature.

Ekspong (E 54) has pointed out the existence of an optical distortion effect. If the magnification varies with the distance from the center of the field (see Section 7.6) then a track somewhat inclined to the x axis will have an apparent curvature even if it is perfectly straight. This has the characteristics of spurious scattering. Such a variation of magnification with position in the field has also been studied by Heckman *et al.* (H-B 60).

Biswas, Peters, and Rama (BPR 55) first suggested that a previously unknown effect caused other emulsion workers, in disagreement with Biswas *et al.*, to find cosmic-ray mass spectra with Li, Be, and B nuclei approximately as abundant as C, N, and O. They studied a type of spurious scattering (s.s.) which could interfere with the indentification of such nuclei.

They attributed the discrepancy to an imperfection of the detecting medium—microscopic dislocations within the emulsion which are too small to interfere with measurements on slow particles. They found it in many kinds of plates, but especially when the track dip angle was more than 2°. They also found it, however, when the supposed distortion was very small. Further work by many people has shown that this effect is present in all emulsions to the magnitude of about half a micron for a cell of 1 mm. It may vary considerably from track to track

in the same emulsion, often being lowest near the glass. It differs in various stacks by a factor of about two. It is thought to originate in processing the emulsion, and to be less in emulsions processed at reduced temperatures. On increasing the cell lenth, the seriousness of the effect is probably reduced. Fischer and Lord (FL 59) observed no further increase in spurious scattering beyond a cell length of 3 mm, while with shorter cells, Brisbout *et al.* (B-J 56) found a $t^{3/2}$-dependence. Biswas, Prasad, and Mitra (BPM 57), on the other hand, found a $t^{0.8}$-dependence from 1 to 3 mm and a $t^{0.5}$-dependence from 3 to 8 mm. Lohrmann and Teucher (LT 56) found proportionality to the cell length with a factor of proportionality 0.042 between the spurious scattering in microns and the cell length in units of 100 μ. Apostolakis, Clarke, and Major (CCM 57) also observed proportionality.

In recent work, D. H. Perkins (D 60) found a 0.8 power law for 18 Bev pions and 24 Bev protons. Its magnitude was 1 μ for 6-mm cells. A. Bonetti (D 60), using similar tracks, found least s.s. when immersed hot-stage development at 23°C was used. He found the s.s. to increase with cell length only up to cells of about 2 mm. Between 3-mm and 6-mm cells, the measured effect was about 0.3 μ on tracks with dip angles of less than 0.3°.

Iursunov *et al.* (ICS 60) have proposed a method to eliminate s.s. which is based on the assumption that the ratio of s.s. measured from second and third differences is independent of cell length.

High-energy accelerators have recently given impetus to the study of s.s. and its relation to the treatment the emulsion has received. Beams from the CERN accelerator have been used, and careful control of the dip angle is usual. In most experiments, the observed s.s. is strongly correlated with the track dip (D 60.3). The opinion now is held that it also is correlated with general disortion, and probably is accentuated in pellicles that have undergone a mounting procedure.

On the other hand, very small s.s. was observed by Dahl-Jensen (D 60.3) when he developed with an inorganic titanious salt. The development was isothermal at 5°C, and the swelling was very small—some 60% while in the developing solution. He noticed, however, that extremely small s.s. was limited to those tracks that were not inclined in the emulsion.

In recent studies of spurious scattering, definitions suggested by E. Dahl-Jensen (G 61) have been used. Since they differ from the notation of this book, these are now given.

$\bar{D}_{\text{meas.}}$ = arithmetic mean of the absolute values of measured second differences.

$\bar{D}_c$ = contribution to second differences due to Coulomb scattering.

$\bar{D}_\epsilon$ = mean second differences due to reading, grain noise, and the irreproducible part of the stage noise.

$\bar{D}_\gamma$ = mean second differences due to the reproducible part of stage noise.

$\bar{D}_{\text{s.s.}}$ = mean second differences due to spurious scattering on a single track.

Then it is assumed that: $\bar{D}^2_{\text{meas.}} = \bar{D}^2_c + \bar{D}^2_\epsilon + \bar{D}^2_\gamma + \bar{D}^2_{\text{s.s.}}$; and that $p\beta = Ks^{3/2}/573\bar{D}_c$. Here K is the scattering factor, s is taken in units of 100 μ, and $p\beta$ is in Bev/c.

When third differences are taken:

$\bar{T}_{\text{meas.}}$ = mean absolute value of the measured third difference. $\bar{T}_c(\approx 3/2\bar{D}_c)$ = contribution in third differences due to Coulomb scattering.

Then also $\bar{T}^2_{\text{meas.}} = \bar{T}^2_c + \bar{T}^2_\epsilon + \bar{T}^2_\gamma + \bar{T}^2_{\text{s.s.}}$ with $\bar{T}^2_\epsilon \approx (10/3)\bar{D}^2_\epsilon$, $\bar{T}^2_\gamma \approx (10/3)\bar{D}^2_\gamma$.

From relative measurements on two parallel tracks with equal $p\beta s$, $\bar{D}^2_{\text{meas.}} = (1/2)\bar{D}^2_r + \bar{D}^2_\gamma + \bar{D}^2_{\text{s.s.}a}$ and $\bar{T}^2_{\text{meas.}} = (1/2)\bar{T}^2_r + \bar{T}^2_\gamma + \bar{T}^2_{\text{s.s.}a}$.

Here $\bar{D}_r$ = mean absolute value of relative second differences measured between two parallel tracks.

$\bar{T}_r$ = mean absolute value of relative third differences.

With these formulas, however, the values found by E. Dahl-Jensen (G 61) for $\bar{D}_{\text{s.s.}a}$ are smaller than those for $\bar{D}_{\text{s.s.}}$. Likewise $\bar{T}_{\text{s.s.}a}$ is smaller than $\bar{T}_{\text{s.s.}}$.

Perhaps agreement on what is being measured will reduce the confusion in this research, which is beset by problems of semantics as well as by uncontrolled variables. We conclude the topic of spurious scattering by citing further reported causes and effects.

J. V. Major (D 60.3) reported that a heat treatment that consisted of holding dry plates at 35°C for 24 hr, followed by slow cooling reduced the general distortion by a factor of three. Pouring on warm glass to prevent too rapid congealing of the gelatin has also been advocated so that the melted emulsion can settle to a uniform thickness (provided the glass is plane and level). An uneven thickness of a pellicle has often been observed, and it is reasonable to assume that such variations can produce strains in the horizontal plane when a pellicle is mounted. The measured thickness variations are seldom less than 2% and are sometimes much more—even 15%. Such nonuniform pellicle thickness obviously also makes satisfactory stack construction difficult.

A. Bonetti (G 61), however, did not observe a significant difference between emulsion poured on glass at 10°C and 20°C. Nonuniform swelling during the presoak also has little effect. On the other hand, it was established (G 61) that nonuniform drying increases the s.s. as does the addition of a plasticizer.

Fear has been expressed that storing of emulsion at a very low temperature may induce spurious scattering. It is thought that ice crystals may form in the emulsion. It has also been reported that there is less s.s. when the pellicle is mounted on the glass upside down. It was suggested by M. Gailloud (D 60.3) that there may be less s.s. if the pellicle is mounted on a support such as gelatin that has some compliance. This would reduce the stress on the lower surface of the emulsion. To help reduce the initial shock of the presoak, B. Peters (D 60.3) suggested immersion in a gradually diluted alcohol solution. There seems also to be no good reason for a stop bath when the emulsion goes into an acid fixing solution. Dahl-Jensen (D 60.3) has suggested that a moderate controlled silver ion concentration in the fix bath is desirable because, (see p. 165-166), corrosion tends to occur if it is too low, and the triply charged complex ion that forms when the concentration is high causes tanning of the gelatin and possible lateral displacements. This apparently has been confirmed by R. Delessert and P. Heinzer (G 61).

Another suspected contributor to s.s. is a fixer temperature that is too low. Track "chopping" has been observed by Dahl-Jensen when the temperature went to— 1.5°C. Chopping is also thought to be caused by insufficient stirring of the fixer. Although no one doubts that the rough handling of the mounting process is a contributor, it is clear that emulsion distortion is not as yet under control in processing, and that it perhaps is still approached with an element of witchcraft. The situation in fact led Dahl-Jensen (D 60.3) to make the following abstract or summary of the proceedings of the Copenhagen meeting on "Problems of Distortion in Nuclear Emulsions and Scattering Measurements at High Energies."

> "Fillet of a fenny snake
> In the cauldron boil and bake:
> Eye of a newt, and toe of a frog,
> Wool of bat, and tongue of dog,
> Adder's fork, and blind-worm's sting,
> Lizard's leg, and owlet's wing,
> For a charm of powerful trouble,
> Like a hell-broth boil and bubble.
>
> All. Double, double toil and trouble;
> Fire, burn; and, cauldron bubble."
>
> (Macbeth, Act. IV, Sc. 1).

8.9.5 Noise Elimination

There are many methods of noise elimination, each of which may be preferable under certain circumstances. The direct method (E 54) is the evaluation of the combined noise in a measurement. Suppose the mean square second difference is measured on the tracks of very high energy particles using the same cell length as for low energy particles. Since $\langle\psi^2\rangle$ and $\langle\chi^2\rangle$ are very small, the measured quantity can be identified with $6\langle\delta^2\rangle$. Any other measurements made in the same emulsion with the same microscope can then be corrected by the amount indicated in the general Eq. (8.4.14). This procedure often is the one to yield the highest accuracy because $\langle\delta^2\rangle$, in principle, can be found with arbitrarily small error by taking many measurements.

Sometimes no really high energy tracks are present, or the necessary calibration measurements have not been made. Then the measurements $y_0, y_1, \cdots y_n$, if combined in more than one way can be used both to eliminate the noise and to evaluate the scattering. When summed over many consecutive cells, some relatively simple combinations of the D''_K are unaffected by the noise. For example:

$$\frac{8}{11}\langle D''^2_K + 3/2 D''_K D''_{K+1}\rangle = \Delta_t^2 \tag{8.9.1}$$

Many other combinations of the D_K, given generally by formula (8.4.13), also can be utilized. When quadratic distortion is present, it disappears in third-differencing (see Section 6.11). This fact enables one either to evaluate the distortion or to eliminate it. If a significant difference between the estimates of Δ from second and third differences is found, the presence of disturbing effects can be suspected.

Besides Eq. (8.9.1), many other combinations of difference products can be used for noise elimination. Thus, for example:

$$\begin{aligned}
\Delta_t^2 &= \frac{8}{11}[\langle D''^2_K\rangle + 3/2\langle D''_K D''_{K+1}\rangle] && \text{(a)}\\
&= \frac{4}{11}[5\langle D''^2_K\rangle - 3/2\langle D'''^2_K\rangle] && \text{(b)}\\
&= [\langle D''^2_K\rangle - 6\langle D''_K D''_{K+2}\rangle] && \text{(c)}\\
&= \frac{1}{4}[5\langle D''^2_K\rangle + 2\langle D'''_K D'''_{K+1}\rangle] && \text{(d)}\\
&= \frac{2}{5}[3\langle D'''^2_K\rangle + 4\langle D'''_K D'''_{K+1}\rangle] && \text{(e)}
\end{aligned} \tag{8.9.2}$$

etc.

Another method, and perhaps the one most frequently used for noise elimination, is that of cell-length variation. Suppose besides the second differences $D''_K = y_K + y_{K+2} - 2y_{K+1}$ from adjacent measurements, cells of length m times the unit cell are used. Then a second difference, $D''_{K,m}$, for example, will be

$$D''_{K,m} = y_K - 2y_{K+m} + y_{K+2m} \tag{8.9.3}$$

This can be expressed as a sum of unit-cell second differences:

$$D''_{K,m} = \sum_{l=0}^{m-2} (l+1)\, D''_{K+l} + \sum_{l=m-1}^{2m-2} (2m-l-1)\, D''_{K+l} \tag{8.9.4}$$

Since $D''_K = \psi_{K+1} + \psi_K + \chi_{K+1} - \chi_K + \delta_K - 2\delta_{K+1} + \delta_{K+2}$, this expression, in turn, can be decomposed into a linear combination of *independent* ψ's, χ's, and δ's.

$$\begin{aligned} D''_{K,m} = &\sum_{l=0}^{m-1} (2l+1)\,(\psi_{K+l} + \psi_{K+m-l-1}) \\ &+ \sum_{l=0}^{m-1} (\chi_{K+2m-l-1} - \chi_{K+l}) \\ &+ \delta_K - 2\delta_{K+m} + \delta_{K+2m} \end{aligned} \tag{8.9.5}$$

The mean value $\langle D''^2_{K,m} \rangle$ is equal to

$$8/3m^3\langle\psi^2\rangle + 6\langle\delta^2\rangle_m \tag{8.9.6}$$

whereas the mean value $\langle D''^2_K \rangle$ is

$$(8/3\langle\psi^2\rangle + 6\langle\delta^2\rangle \tag{8.9.7}$$

The noise $\langle\delta^2\rangle_m$ of the m-fold cell is subscripted so that the possibility will not be overlooked that the noise may depend on cell length. Then

$$\Delta^2 = 8/3\langle\psi^2\rangle = \frac{\langle D''^2_{K,m}\rangle - \langle D''^2_K\rangle}{m^3 - 1} - \frac{6[\langle\delta^2\rangle_m - \langle\delta^2\rangle]}{m^3 - 1} \tag{8.9.8}$$

When it has been established that $\langle\delta^2\rangle_m = \langle\delta^2\rangle$, this procedure largely eliminates the noise, but the dependence of the scattering factor on cell length complicates the problem of accurate noise elimination by

variation of cell length. Because of this error, the difference-product method using Eq. (8.9.2) with cells of a single size may be preferable. If it is decided to employ the method of varying cell length, a correction for the change in scattering factor has been published by Widgoff (W 61). The approximate effect of her correction is to make the exponent of m in Eq. (8.9.8) equal to 3.13 rather than to 3.

8.10 Evaluation of Error in Multiple Scattering Measurements

8.10.1 Sources of Error

A reason for measuring the multiple scattering of a track in emulsion is to estimate the quantity $p\beta/z$. One calculates this from $p\beta/z = (K/573D_t)t^{3/2}$. Here D_t and the cell length, t, are in microns. Unless the track is inclined to the x axis, the error in t is ordinarily negligible. The error in K is systematic, and may be unknown, but also usually is negligible compared to the statistical error. The scattering factor K was discussed in Section 8.7; often it may carry a subscript to indicate a cut off.

The remaining uncertainties are in D_t. Some are systematic, and statistical errors are always present. Only the resultant of many measurements has good reliability. As compared with range measurements, for example, multiple scattering data yield only crude estimates of particle momenta. Still, when the particle does not come to rest and the grain density is near the minimum or unreliable, multiple scattering provides invaluable information. Virtually as important as a careful measurement, however, is the correct evaluation of a confidence interval for it. Compared with the statistical error, the systematic errors are generally small. We shall concern ourselves with evaluating the error when various methods of noise elimination are employed.

The measurable quantities, D_K^r, given by Eq. (8.4.13) are made up of linear combinations of the scattering moments and δ's. Each is, therefore, a random variable of expectation value zero. The uncertainty in the root-mean-square magnitude of a single measurement is as great as the estimate of the variable itself. To measure such a quantity requires that one find the average value from observations at many points with indices 0, 1, 2, $\cdots K, \cdots \nu$, along a track. The uncertainty is then reduced by a factor $\approx \nu^{1/2}$, but to know the magnitude of one of these quantities (including the noise) to 10% requires the order of 100 *independent* measures of it.

Estimates of the error that were too low because the dependent character of the observations was not realized, led some early experi-

menters to be too optimistic in their quotations of multiple scattering accuracy.

The statistics of multiple scattering measurements has been studied intensively by Moyal (M 50), d'Espagnat (D 51.1, D 52.1), Molière (M 55), Solntseff (S 57.2, S 58.5), and others. The approach is generally that of the "MME" (Moyal, Molière, d'Espagnat) method, which recognizes that one is here concerned with two types of statistical variables, the "noise" and the "signal." Furthermore, successive measurements are not independent, and are correlated in different ways for the two kinds of variables. The problem becomes very complicated in the general case. In this book, by introducing the quantities ψ and χ, however, which are independent of each other and of the δ's, we reduce the difficulty of the problem and the calculations become straightforward. They remain somewhat tedious, nevertheless.

8.10.2 Statistical Error in the Difference-Product Method

The considerations which enable one to evaluate the error in any special case will perhaps best be illustrated by the detailed calculation of an example in which we employ the new variables. Suppose we consider

$$S = \sum_K [D''^2_K + (3/2)\, D''_K D''_{K+1}] \tag{8.10.1}$$

the average value of which is equal to $(11/8)\nu\Delta_l^2$, where ν is the number of cells included in the sum. The quantity S has been constructed so that in the average value, noise has been eliminated. A typical second difference, when expressed in terms of independent variables, is the sum of seven terms:

$$D''_K = \psi_{K+1} + \psi_K + \chi_{K+1} - \chi_K + \delta_K - 2\delta_{K+1} + \delta_{K+2} \tag{8.10.2}$$

When it is squared, there remain just seven terms that do not have average values of zero, namely,

$$\psi^2_{K+1} + \psi^2_K + \chi^2_{K+1} + \chi^2_K + \delta^2_K + 4\delta^2_{K+1} + \delta^2_{K+2} \tag{8.10.3}$$

In addition, there are twenty-one terms that average out to zero but must not be dropped at this stage. On collecting the contribution of a single cell to the sum of the squares of the second differences obtained from many consecutive measurements, seventeen terms remain. Similarly, the contribution of one cell to the sum $3/2\,\Sigma_K D''_K D''_{K+1}$ over many consecutive

cells consists of twenty-two terms. The net contribution, S_l, of one cell to S is:

$$\begin{aligned} S_l = {} & 7/2\psi_l^2 + \tfrac{1}{2}\chi_l^2 + 5\psi_l\psi_{l+1} - 2\psi_{l+1}\chi_l + 3/2\psi_l\psi_{l+2} \\ & + \tfrac{1}{2}\psi_{l+2}\delta_l - 2\psi_{l+1}\delta_l - 2\psi_l\delta_l + 2\psi_l\chi_{l+1} \\ & + 3/2\psi_l\chi_{l+2} + \chi_l\chi_{l+1} - 3/2\psi_{l+2}\chi_l - 3/2\chi_l\chi_{l+2} \\ & + \tfrac{1}{2}\psi_l\delta_{l+1} - 5/2\chi_{l+2}\delta_l + 5/2\chi_l\delta_{l+1} - 3/2\chi_l\delta_{l+2} \\ & + 3/2\psi_{l+3}\delta_l + 3/2\chi_{l+3}\delta_l + 5/2\delta_l\delta_{l+1} + 3/2\delta_l\delta_{l+3} \\ & - 4\delta_l\delta_{l+2} + 3/2\psi_l\delta_{l+2} \end{aligned} \tag{8.10.4}$$

The mean value $\langle S_l \rangle$ of S_l is

$$\langle S_l \rangle = 7/2\langle\psi^2\rangle + 1/2\langle\chi^2\rangle = 11/3\langle\psi^2\rangle = 11/8\Delta_t^2 \tag{8.10.5}$$

and

$$\langle S_l \rangle^2 = 121/9\langle\psi^2\rangle^2 \tag{8.10.6}$$

Then the variance, $\langle S_l^2\rangle - \langle S_l\rangle^2 \equiv \sigma_l^2$, of S_l is

$$\sigma_l^2 = \frac{49}{4}\langle\psi^4\rangle + \frac{1}{4}\langle\chi^4\rangle + \frac{55}{3}\langle\psi^2\rangle^2 + \frac{56}{3}\langle\psi^2\rangle\langle\delta^2\rangle + \frac{49}{2}\langle\delta^2\rangle^2 \tag{8.10.7}$$

In the Gaussian approximation

$$\langle\psi^4\rangle = 9\langle\chi^4\rangle = 3\langle\psi^2\rangle^2 = (27/64)\,\Delta_t^4 \tag{8.10.8}$$

Then the estimate of the variance becomes:

$$\sigma_l^2 = \frac{331}{6}\langle\psi^2\rangle^2 + \frac{56}{3}\langle\psi^2\rangle\langle\delta^2\rangle + \frac{49}{2}\langle\delta^2\rangle^2 \tag{8.10.9}$$

When there are ν cells in S, its variance, Σ^2, is $\nu\sigma_l^2$ and the mean value of S is

$$\nu\langle S_l\rangle = (11/8)\,\nu\Delta_t^2 \tag{8.10.10}$$

The relative uncertainty in the mean absolute scattering angle $\bar{\alpha}$ is one-half that in S. We can state then, finally, that the standard deviation σ_α of the angle measurement $\bar{\alpha}$ is

$$\sigma_\alpha = (2\nu)^{-1/2}\,\bar{\alpha}(2.052 + 2.777\lambda + 14.58\lambda^2)^{1/2} \tag{8.10.11}$$

In this expression $\lambda = \langle\delta^2\rangle/(t^2\langle\phi^2\rangle)$. It is the same as the λ of d'Espagnat.

The optimum cell length when one uses the difference-product method of noise elimination, as first shown by d'Espagnat (D 52.1), is found from the condition that $\lambda = 0.134$. Then

$$\frac{\sigma_\alpha}{\bar{\alpha}} = \frac{1.15}{(\nu)^{1/2}} \tag{8.10.12}$$

When plenty of track is available, and only time limits the accuracy obtainable, then a cell long enough so that the mean absolute second difference is at least four times the noise may be used. If this is done usually the noise can be neglected in calculating the mean value. The relative error in the mean second difference then is $3/4\nu^{1/2}(1 + 4\lambda + 32\lambda^2)^{1/2}$. This applies only after subtracting the noise, when it is not completely negligible. The optimum length of a cell when a limited amount of track is available, but from which the noise has been subtracted out, is given by $\lambda = 0.0725$. The relative error is $0.9\nu^{-1/2}$ when this cell length is used.

The writer's method for calculating the error was worked out as an alternative to the conventional method of d'Espagnat-Molière. Their methods, which use more difficult mathematics, may be preferred by some, although the calculations are long in any case. They define

$$R = t \sum_i \sum_j b_{ij} D_i'' D_j''$$

the bilinear form encountered in the elimination of noise. Then b_{ij} and $A_{Kl} \equiv \langle D_K'' D_l'' \rangle$ are matrices. The mean value $\langle R \rangle$ is found from $\langle R \rangle = \text{Trace } (bA)$ and $\langle R^2 \rangle - \langle R \rangle^2 = 2 \text{ Trace } (bAbA)$, with $b_{ii} = 1$, $b_{i,i\pm1} = 3/4$, $b_{iK} = 0$, $| i - K | > 1$.

The A_{Kl} are found from Eq. (8.4.14). The above calculations are all based on the assumption of complete overlapping of cells.

8.10.3 Overlapping Cells

We obtain the maximum amount of information from a track segment by overlapping the cells. Both the quantities $y_{K+1} - 2y_{K+2} + y_{K+3}$ and $y_K - 2y_{K+1} + y_{K+2}$ are used in calculating mean second differences, although they have ordinates y_{K+1} and y_{K+2} in common. The error calculation becomes very complex when higher differences are evaluated. Third differencing yields four quantities having at least one ordinate in common:

$$y_K - 3y_{K+1} + 3y_{K+2} - y_{K+3}$$
$$y_{K+1} - 3y_{K+2} + 3y_{K+3} - y_{K+4}$$
$$y_{K+2} - 3y_{K+3} + 3y_{K+4} - y_{K+5}$$

and

$$y_{K+3} - 3y_{K+4} + 3y_{K+5} - y_{K+6}$$

When they are all used in averaging, as is most common, one speaks of complete overlapping.

D'Espagnat has given error estimates for some cases.

As a quick practical method for estimating error in second difference measurements with overlapping cells it is common to quote the error on the assumption that two-thirds of the cells are independent.

8.10.4 Variation of Cell Length

For results obtained in a comprehensive study of the method of variation of cell size, we refer to the work of diCorato, Hirschberg, and Locatelli (DHL 56).

The noise-corrected mean absolute second difference (the scattering sagitta) was found from second differences as follows:

$$D = \left(\frac{\langle | D'' |_m \rangle^2 - \langle | D'' |_1 \rangle^2}{m^3 - 1}\right)^{1/2} \tag{8.10.13}$$

The same quantity was also calculated from third and fourth differences. The formulas are:

$$D = \left[\frac{\langle | D''' |_m \rangle^2 - \langle | D''' |_1 \rangle^2}{(3/2)\,(m^3 - 1)}\right]^{1/2}$$
$$D = \left[\frac{\langle | D'''' |_m \rangle^2 - \langle | D'''' |_1 \rangle^2}{4(m^3 - 1)}\right]^{1/2} \tag{8.10.14}$$

In accord with the definition Eq. (8.9.3), the subscript m means that the quantity was calculated using cells of m times the unit cell. Cut off at four times the resultant mean was applied by diCorato *et al.* As noted above the method of noise elimination between cells of different lengths is inapplicable when the noise depends on the cell length. The noise for any particular cell length can be determined, however, by the difference-product method and the measurements corrected accordingly. The values of D derived with different cell lengths should then be compared for consistency.

If (σ_D/D) is the standard deviation of D divided by D, then for ν cells the error can be written $\sigma_D/D = c(\nu)^{-1/2}$, and c can be discussed as a function of signal to noise ratio D_t/D_0. The formulas are independent of cell length and the signal D in the ratio, therefore, is left unsubscripted. The noise D_0, moreover, consists chiefly of the term $[(12/\pi)\,\langle\delta^2\rangle]^{1/2}$

which does not vary with cell length. It has a typical value of 0.15 μ. The error coefficient, c, falls at first as the signal-to-noise ratio increases; for large values of D/D_0 it becomes constant. For second differences it is (BDS 58) $c'' = [2.03 + 0.138(D_0^2/D^2) + 0.0402(D_0^4/D^4)]^{1/2}$, and for third differences: $c''' = [3.6 + 0.096(D_0^2/D^2) + 0.003(D_0^4/D^4)]^{1/2}$. These refer to measurements made with completely overlapping cells. If ν exceeds 100 and D_0 is 0.15 μ, then the optimum cell length for second differencing using cells of double length for noise elimination is $t \approx 2.3(p\beta)^{2/3}$, and for third differencing $t \approx 1.8(p\beta)^{2/3}$. The cell length t is measured in microns and $p\beta$ in Mev/c. If the number of cells lies between 40 and 100, then D/D_0 should be kept larger than 1.4, and if the number of cells is less than 20 the signal-to-noise ratio must be kept above 1.6.

The noise has a negligible effect when the cell length is increased sufficiently. This is usually defined to be at the point where $D/D_0 = 4$ for second differences, and $D/D_0 = 5$ for third. For these conditions, the optimum cell length for second differencing is 20.6 $(D_0 p\beta)^{2/3}$, and for third differencing it is $25(D_0 p\beta)^{2/3}$. In these expressions, lengths are in microns and $p\beta$ in Mev/c. The error coefficients are (BDS 58): $c'' = [0.95 + 1.13(D_0^2/D^2) + 2.49(D_0^4/D^4)]^{1/2}$ and $c''' = [1.53 + 6.45 \times (D_0^2/D^2) + 10.33(D_0^4/D^4)]^{1/2}$.

For comparison with formulas containing d'Espagnat's λ, we note that in the Gaussian approximation (D 51.1).

$$\lambda = \left(\frac{1}{3}\frac{D_0}{D}\right)^2 \tag{8.10.15}$$

DiCorato *et al.* carried out extensive measurements on tracks of π mesons and protons. These data were compared with the theory.

Using second differencing on proton tracks they found $c = 1.46 \pm 0.18$, when theory predicted 1.46. On pion tracks they found 1.67 ± 0.18 when theory predicted 1.46.

When they used third differences they found for protons that c was 1.86 ± 0.24 when the theoretical value was 1.56. For pions they measured 2.00 ± 0.22 when they expected 1.56.

Fourth differencing gave experimental values of c for protons and pions respectively of 2.20 ± 0.28 and 2.70 ± 0.35.

The calculated D from third differences on fast tracks was 1.06 ± 0.02 times that obtained from second differences. Presumably this exceeds unity because the differences are not normally distributed.

For elimination of regular distortions they suggest using the formula

$$D = \frac{1}{1.06}\left[\frac{\langle |\, D''' \,|_m \rangle^2 - \langle |\, D''' \,|_1 \rangle^2}{(3/2)(m^3 - 1)}\right]^{1/2} \tag{8.10.16}$$

It does not seem to the writer that the factor 1.06 can be universally applicable; it is given here merely as an empirical correction factor. The factor is symbolized by F.

8.10.5 Noise Level Known

According to Ekspong (E 54), to gain the optimum information from a segment of track when the noise level is known, a cell length giving a signal-to-noise ratio of 2.1 is best. The cell length may be increased until a signal-to-noise ratio of 3.7 is reached without increasing the error by more than 10%. At this point the systematic error remaining if the noise is not eliminated is only 1%, and the amount of work is greatly reduced.

8.11 Scattering Behavior of Stopping Particles

When a particle is brought to rest in emulsion its scattering sagitta for a given cell length increases as the velocity decreases. A functional connection exists between the cell length and the residual range that will maintain the scattering sagitta statistically constant. The approximate constancy of the sagitta is not destroyed if the track of a particle with a different mass is measured in the same way, but the magnitude of the constant will vary with the mass.

We define a mean scattering sagitta $\bar{D}_c$ by

$$\bar{D}_c = \frac{K_c z t^{3/2}}{573 p\beta} \tag{8.11.1}$$

In a velocity interval extending from about $\beta = 0.05$ to 0.40, and for cells of 10-100 μ $(K_c/p\beta)$ is reasonably well approximated by

$$K_c/p\beta = \alpha M^{m-1} z^{\epsilon-2m} R^{-m} t^{\epsilon} \tag{8.11.2}$$

Here m is a number near 0.58, M and z are particle mass and charge in units of the proton, R is the residual range in microns, t is the cell length, and, for this velocity interval, ϵ is a small number approximately equal to 0.087. A scattering sagitta in a small interval of velocity and cell length, therefore, can be expressed functionally by

$$\bar{D}_c = a M^{m-1} z^{\epsilon-2m+1} R^{-m} t^{\epsilon+3/2} \tag{8.11.3}$$

where a is a constant. This means that if measurements are made at residual ranges R using a cell t which is adjusted so that $R^{-n} t^{\epsilon+3/2}$

TABLE 8.11.1

TABLE OF RANGES FOR HALF π CELLS

No.	R	No.	R	No.	R	No.	R
1	48	51	372	101	907	151	1 616
2	52	52	381	102	920	152	1 632
3	56	53	390	103	932	153	1 648
4	60	54	399	104	945	154	1 664
5	64	55	408	105	958	155	1 680
6	69	56	417	106	971	156	1 696
7	73	57	426	107	984	157	1 712
8	78	58	436	108	997	158	1 728
9	82	59	445	109	1 010	159	1 744
10	87	60	455	110	1 023	160	1 760
11	92	61	464	111	1 036	161	1 776
12	97	62	474	112	1 050	162	1 793
13	102	63	483	113	1 063	163	1 809
14	108	64	494	114	1 077	164	1 826
15	113	65	504	115	1 090	165	1 842
16	119	66	514	116	1 104	166	1 859
17	124	67	524	117	1 117	167	1 875
18	130	68	534	118	1 131	168	1 892
19	136	69	544	119	1 144	169	1 909
20	142	70	554	120	1 158	170	1 926
21	148	71	564	121	1 172	171	1 943
22	154	72	575	122	1 186	172	1 960
23	160	73	585	123	1 200	173	1 977
24	167	74	596	124	1 214	174	1 995
25	173	75	606	125	1 288	175	2 012
26	180	76	617	126	1 242	176	2 030
27	186	77	627	127	1 256	177	2 047
28	193	78	638	128	1 271	178	2 065
29	200	79	649	129	1 285	179	2 082
30	207	80	660	130	1 300	180	2 100
31	214	81	671	131	1 314	181	2 117
32	221	82	682	132	1 329	182	2 135
33	228	83	692	133	1 343	183	2 153
34	236	84	704	134	1 358	184	2 171
35	243	85	715	135	1 372	185	2 189
36	251	86	727	136	1 387	186	2 207
37	258	87	738	137	1 402	187	2 225
38	266	88	750	138	1 417	188	2 243
39	273	89	761	139	1 432	189	2 261
40	281	90	773	140	1 447	190	2 279
41	289	91	785	141	1 462	191	2 297
42	297	92	797	142	1 477	192	2 315
43	305	93	809	143	1 492	193	2 333
44	313	94	821	144	1 507	194	2 352
45	321	95	833	145	1 522	195	2 370
46	330	96	845	146	1 538	196	2 389
47	338	97	857	147	1 553	197	2 407
48	347	98	870	148	1 569	198	2 326
49	355	99	882	149	1 584	199	2 444
50	364	100	895	150	1 600	200	2 463

TABLE 8.11.1 (*cont'd.*)

No.	*R*	No.	*R*	No.	*R*	No.	*R*
201	2 481	251	3 485	301	4 612	351	5 852
202	2 500	252	3 507	302	4 636	252	5 878
203	2 518	253	3 528	303	4 659	353	5 904
204	2 537	254	3 550	304	4 683	354	5 930
205	2 555	255	3 571	305	4 707	355	5 956
206	2 574	256	3 593	306	4 631	356	5 982
207	2 593	257	3 614	307	4 755	357	6 008
208	2 612	258	3 636	308	4 779	358	6 035
209	2 631	259	3 658	309	4 803	359	6 061
210	2 650	260	3 680	310	4 827	360	6 088
211	2 669	261	3 702	311	4 851	361	6 114
212	2 689	262	3 724	312	4 876	362	6 141
213	2 708	263	3 746	313	4 900	363	6 167
214	2 728	264	3 768	314	4 925	364	6 194
215	2 747	265	3 790	315	4 949	365	6 220
216	2 767	266	3 812	316	4 974	366	6 247
217	2 786	267	3 834	317	4 998	367	6 274
218	2 806	268	3 856	318	5 023	368	6 301
219	2 825	269	3 878	319	5 407	369	6 328
220	2 845	270	3 901	320	5 072	370	6 355
221	2 865	271	3 923	321	5 096	371	6 382
222	2 885	272	3 946	322	5 121	372	6 490
223	2 905	273	3 968	323	5 145	373	6 436
224	2 925	274	3 991	324	5 170	374	6 463
225	2 945	275	4 013	325	5 194	375	6 490
226	2 965	276	4 036	326	5 129	376	6 518
227	2 985	277	4 058	327	5 244	377	6 545
228	3 005	278	4 081	328	5 269	378	6 573
229	3 025	279	4 103	329	5 294	379	6 600
230	3 046	280	4 126	330	5 319	380	6 628
231	3 066	281	4 148	331	5 344	381	6 655
232	3 807	282	4 171	332	5 369	382	6 683
233	3 107	283	4 194	333	5 394	383	6 710
234	3 128	284	4 217	334	5 419	384	6 738
235	3 148	285	4 240	335	5 444	385	6 765
236	3 169	286	4 263	336	5 969	386	6 793
237	3 190	287	4 286	337	5 494	387	6 820
238	3 211	288	4 309	338	5 520	388	6 848
239	3 232	289	4 332	339	5 545	389	6 875
240	3 253	290	4 355	340	5 571	390	6 903
241	3 274	291	4 378	341	5 596	391	6 930
242	3 295	292	4 401	342	5 622	392	6 958
243	3 316	293	4 424	343	5 647	393	6 985
244	3 337	294	4 448	344	5 673	394	7 013
245	3 358	295	4 471	345	5 698	395	7 040
246	3 379	296	4 495	346	5 724	396	7 068
247	3 400	297	4 518	347	5 749	397	7 095
248	3 421	298	4 542	348	5 775	398	7 123
249	3 442	299	4 565	349	5 800	399	7 150
250	3 464	300	4 589	350	5 826	400	7 178

remains constant, $\bar{D}_c$ will be statistically constant. It also implies that when $R^{-n}t^{\epsilon+3/2}$ is kept constant, measurement of $\bar{D}_c$ may enable one to identify the particle that produced the track, for then $M^{1-n}z^{2n-1-\epsilon}$ is statistically constant. It may be found to correspond to the mass and charge of a known particle. The charge often is obvious from the appearance of the track; then the measurement provides a mass estimate.

A number of investigators (HIS 53, G 55.2, LPP 53, DGH 54, ADF 58) have put forward scattering cell schedules designed to maintain a constant sagitta for a mass measurement. They are of varying degrees of refinement. One of the most carefully prepared tables of scattering cells is that of Dilworth, Goldsack, and Hirschberg (DGH 54) which has been reproduced as Table 8.11.1.

What is tabulated are residual ranges at which ordinates y_K are to be measured. The cell lengths chosen, though, are half as long as the optimum cell for a π meson, about one-third of the optimum cell for K particles, and about one-fourth the optimum for a proton. The shorter cells are for use in noise elimination, and for overlap to obtain more information from a limited length of track.

The basis for constructing this cell schedule is the assumed constancy of a standard sagitta, D_s, given by

$$D_s = 1.99 \times 24 \times R^{-0.58} M^{-0.42} Z^{-0.16} t^{3/2} \tag{8.11.4}$$

The measured sagitta, $\bar{D}_c$, is, by the definition of K_c, the quantity in Eq. (8.11.1). (Dilworth *et al.* use the symbol D for $\bar{D}_c$ and K_s for our K_c.) The measurement consists of finding the average $\bar{D}_c$ over many cells. Then, with $\bar{\lambda}$ a number near unity, $\bar{D}_c/\bar{\lambda} = D_s$. Using this numerical value of D_s, Eq. (8.11.4) can be solved for M.

The device of introducing $\bar{\lambda}$ at this point is an advantage of this method. The problem remains of evaluating $\bar{\lambda}$, which deviates from unity because many approximations are involved in setting the expression of Eq. (8.11.4), constant. Dilworth *et al.* give curves for $\bar{\lambda}$, which, considering the crudeness of Eq. (8.11.4), can be sufficiently well represented by:

$$\bar{\lambda} = 0.97 + \frac{0.0145}{M} + \left(4.4 + \frac{0.7}{M}\right) \times 10^{-5} n \tag{8.11.5}$$

Here n is the number of half π cells (the cells of Table 8.11.1) and M is the particle mass in units of the proton. Since M is usually the quantity to be found, one must determine it by successive approximations.

Although $\bar{\lambda}$ was evaluated as well as practical in the study of Dilworth

et al., better information on the scattering factor and on the range-energy relation will enable one to make improvements on Eq. (8.11.5) in the future.

DiCorato *et al.* (DHL 56) give curves of $\bar{\lambda}$ from a range-energy curve of Baroni *et al.* (B-M 54). Recent range measurements by the writer and his collaborators indicate that 0.60 would be a better exponent for R than 0.58 at low velocities. This fact and failure to include the cell length and the exponent ϵ in Eq. (8.11.4) are further reasons why more calibration data are needed. The important advantage of the method of Dilworth *et al.* is not that the cell scheme is necessarily the best, but that it may be calibrated for application without revision of the cell scheme. Before undertaking serious mass measurements by this method it is advisable for anyone to scatter several particles of known masses. By this means he gains training, he calibrates the method, and he obtains a measure of the statistical error.

The cell scheme of Dilworth *et al.* has been tested or calibrated in this way with the tracks of known particles by diCorato, Hirschberg, and Locatelli (DHL 54). They measured proton tracks of average length 12,000 μ, and pion tracks of average length 4900 μ, using the cells of Table 8.11.1. For pions they eliminated noise between the tabulated cells and double cells. Noise was eliminated between double and quadruple cells on proton tracks. In each case the noise was about 0.14 μ. Cut off at $4\bar{D}_c$ was made. The mean sagitta, reduced to pion cells was $0.224 \pm 0.005\,\mu$ for protons, and $0.482 \pm 0.007\,\mu$ for pions. The estimated mass ratio, therefore, is 6.20 ± 0.4, compared with the accepted value of 6.7. The scattering factor came out about 12% higher than expected.

Third differences were also calculated, and those affected by the second difference cut off were discarded. The sagittas obtained were: $\bar{D}_3 = 0.236 \pm 0.006\,\mu$ for protons, and $\bar{D}_3 = 0.491 \pm 0.012\,\mu$ for pions. Since these are both larger than the corresponding values from second differencing, they tend to confirm the need for the factor 1.06 in Eq. (8.10.16).

For comparison, Glasser (G 55) derived the relationship

$$\bar{D} = (19.0 \pm 0.3)\,[R^{-(0.607\pm0.016)}\,M^{-(0.393\pm0.016)}]\left(\frac{t}{50}\right)^{3/2} \qquad (8.11.6)$$

by measurements on many pions and protons of residual range 2500 μ. He has developed cell schemes based on his empirical data.

The quantities $\langle\phi^2\rangle$ and $\langle y^2\rangle$, found in Section 8.5, were calculated by Fermi only for particles so energetic that their momenta could be

treated as constant. They can be calculated for particles coming to rest in matter as follows: From Eq. (8.4.1) $d\langle\theta^2\rangle/dt = \theta_s^2$, but when θ_s is not constant, its dependence on t must be expressed explicitly before this equation can be integrated. Now $\theta_s = K_0 z/p\beta$ with K_0 the appropriate scattering factor. An empirical expression (Section 10.3) for the dependence of $p\beta$ on the residual distance $R_p - t$ remaining to be traversed before coming to rest is

$$p\beta \approx 0.44 z^{6/5} M^{2/5} (R_p - t)^{3/5} \text{ Mev}/c$$

for nonrelativistic velocities. Then

$$\theta_s = (K_0/0.44)\, z^{-1/5} M^{-2/5} (R_p - t)^{-3/5}$$

and

$$d\langle\theta^2\rangle/dt = K_0/0.44)^2\, z^{-2/5} M^{-4/5} (R_p - t)^{-6/5}$$

The mean square scattering angle after traversing a path t therefore is

$$\langle\theta^2\rangle = 2\langle\phi^2\rangle = \alpha z^{-2/5} M^{-4/5}[(R_p - t)^{-1/5} - R_p^{-1/5}] \qquad (8.11.7)$$

with $\alpha = 5(K_0/0.44)^2$.

The pole at $t = R_p$ signifies that as a particle comes to rest, its direction of motion becomes undefined.

The calculation of $\langle y^2\rangle$ is somewhat less straightforward. On putting Δt for the cell length in Eq. (8.4.6), we obtain

$$y_{K+1} = y_K + \phi_K \Delta t + \psi_K + \chi_K + \delta_{K+1} - \delta_K$$

Then we can construct

$$\frac{[\langle y_{K+1}^2\rangle - \langle y_K^2\rangle] - [\langle y_K^2\rangle - \langle y_{K-1}^2\rangle]}{(\Delta t)^2} = \frac{2\langle y_K\phi_K - y_{K-1}\phi_{K-1}\rangle}{\Delta t} + \frac{\Delta t}{2}[\langle\theta_s^2\rangle_{K+1} - \langle\theta_s^2\rangle_K]$$

In the limit as $\Delta t \to 0$

$$\frac{d^2\langle y^2\rangle}{dt^2} = 2\langle\phi^2\rangle = \langle\theta^2\rangle \qquad (8.11.8)$$

Therefore, we can use Eq. (8.11.7) to write

$$\frac{d^2\langle y^2\rangle}{dt^2} = \alpha z^{-2/5} M^{-4/5}[(R_p - t)^{-1/5} - R_p^{-1/5}]$$

On integrating from 0 to t we find $d\langle y^2\rangle/dt(= 2\langle y\phi\rangle)$.

$$\frac{d\langle y^2\rangle}{dt} = \alpha z^{-2/5} M^{-4/5} \left[\frac{5}{4} R_p^{4/5} - \frac{5}{4}(R_p - t)^{4/5} - R_p^{-1/5} t\right]$$

Then on integrating a second time

$$\langle y^2\rangle = (\alpha/2) z^{-2/5} M^{-4/5} \left[\frac{5}{2} R_p^{4/5} t + \frac{25}{18}(R_p - t)^{9/5} - \frac{25}{18} R_p^{9/5} - R_p^{-1/5} t^2\right]$$

When $t = R_p$, the terminal value of $\langle y^2\rangle$ is found

$$\langle y^2\rangle_{\text{term}} = (\alpha/18) z^{-2/5} M^{-4/5} R_p^{9/5} \tag{8.11.9}$$

A precise determination of α has not been carried out. A simple means for estimating it is by observing $\langle y^2\rangle$ of tracks terminating in emulsion. The root-mean-square displacement of the termini of muons originating in the decay of π^+ mesons at rest is suitable. Hester Yee made some measurements of this displacement and found it to be closely Gaussian. This displacement was determined to be $89 \pm 5\ \mu$. The corresponding value of R_p is $572\ \mu$. Using the above data, we find $K_0 = 0.113$, when the proton is chosen to be the unit of mass and of charge, the unit of length is $1\ \mu$, and momenta are measured in Mev/c.

Finally we have

$$\langle\theta^2\rangle \approx (1/3)(z^{1/2}M)^{-4/5}[(R_p - t)^{-1/5} - R_p^{-1/5}] \tag{8.11.10}$$

and

$$\langle y^2\rangle \approx (1/6)(z^{1/2}M)^{-4/5}[(5/2) R_p^{4/5} t + (25/18)(R_p - t)^{9/5} - (25/18) R_p^{9/5} - R_p^{-1/5} t^2] \tag{8.11.11}$$

In Chapter 10 we apply these results to correct particle-range measurements for the effect of scattering.

8.12 Equipment for Scattering Measurements

In Section 8.8 we mentioned types of goniometers that in the past were used in track-tangent multiple scattering measurements. We shall now briefly review features of typical equipment, commercially and custom built, that have been developed for scattering measurements using the

coordinate method. A detailed and authoritative description of such equipment has been given by Hodges (H 60).

8.12.1 Stage Motion

One of the primary considerations is that the stage noise be low. For high energy physics, room enough for a large plate, at least 30 × 30 cm, to be mounted in any orientation on the stage also has become an important requirement. Some workers have demanded a long screw providing large displacements. While convenient, this seems to the writer to be an unnecessary luxury. Tracks rarely stay in a pellicle more than 1 or 2 cm, and a noise-free stage motion of 2 or 3 inches is enough. Even if rare good fortune kept a track in a single pellicle for a distance greater than this, no data need be lost. When the plate is shifted to continue the scattering, one merely overlaps slightly the segment of track already measured. Even if a track were to stay in the pellicle for several centimeters, it is most unlikely that it would not in that length

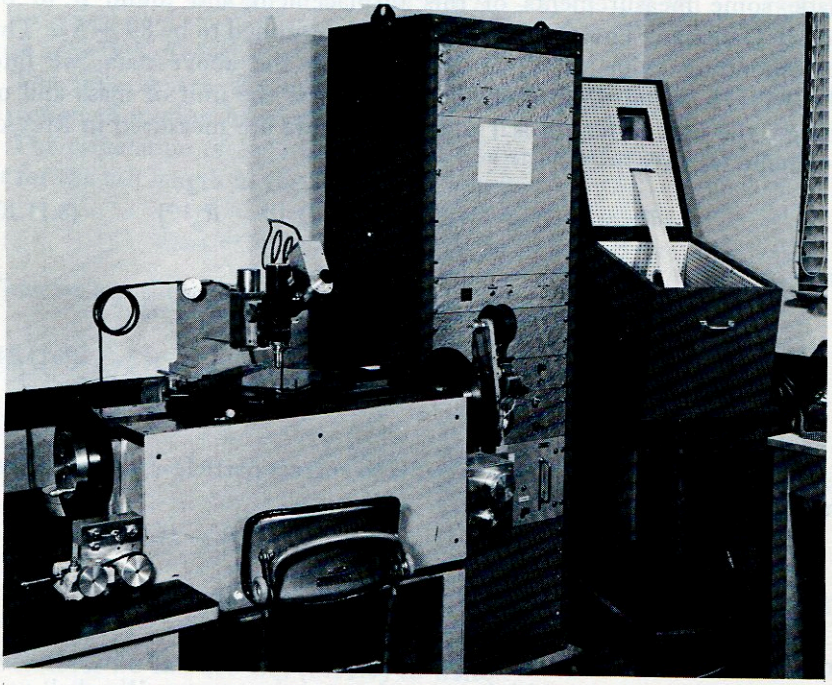

FIG. 8.12.1. A scattering microscope of Brower made for Dr. G. Goldhaber. It provides a large range of displacement, automatic cell schedules, and automatic calculation of second differences (IDLRL).

scatter sufficiently to leave the field or at least to depart somewhat from the center. If it does not cross near the diameter of the field, it must be shifted back to the center if it is not to suffer from the nonuniform magnification noise discussed by Ekspong (E 54).

There may be occasions, nevertheless, when a stage having a large range of travel is desired. One has been described by Zorn (Z 58). A number of stages made by William Brower also have long ways and lead screws (see Fig. 8.12.1).

In the event that tracks are to be measured that are not quite parallel to the stage motion, the cell lengths must be accurate also. Statistical fluctuation of the cell length around an accurately known mean value causes only small errors for tracks closely parallel to the x axis, but for a track inclined with respect to the axis by an angle ϕ, the ordinate error, Δ, introduced by an error ϵ in the cell length is $\epsilon \tan\phi$. That this can be serious is easily seen by an example. Should ϵ be the order of 5 μ and ϕ only as much as 5°, then the noise from this source would be $\approx 0.35\ \mu$. Even an error of only 1 μ in the cell length introduces a serious component of noise into measurements on somewhat inclined tracks.

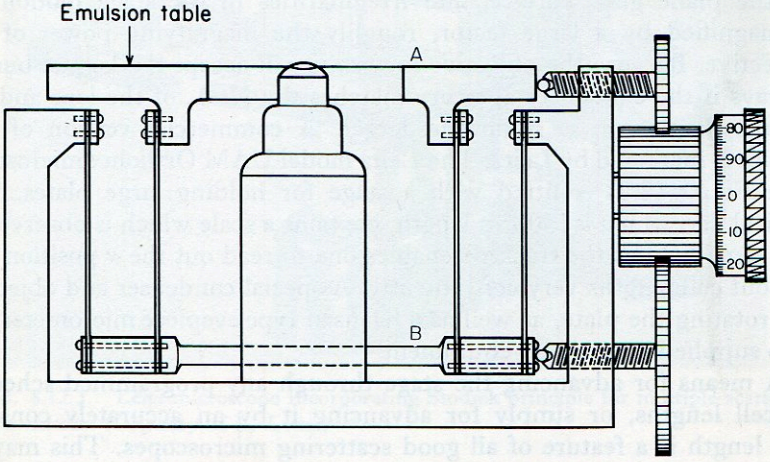

FIG. 8.12.2. Principle of the Cosyns' parallel blade stage support (IDLRL).

One of the most satisfactory principles of stage construction for low noise was first described by Cosyns (C 51). The stage, as shown in Fig. 8.12.2 was mechanically supported on leaf springs, the bending of which permits it to move in the x direction, but the rigidity of which prevents y motion. The construction with two vertical members of equal com-

pliance at each end is designed to prevent motion along the z direction when the stage is displaced along the x direction.

In the illustration, Fig. 8.12.2, the displacement of the lower member is made just half as great as that of the stage proper. Forces in the x direction are applied through ball bearing contacts so that transverse forces are not transmitted to the stage. This principle is in current use on some of the best scattering microscopes.

Selected ball bearings running in carefully lapped ways have been tried for scattering stages, but have not proven completely satisfactory. Probably the small area of contact of the ball contributes to this. Sliding hand-lapped ways with large areas of contact are made by Brower, for example, that are sufficiently good for the most exacting scattering measurements.

Stodiek (S 55) has developed a device for making scattering measurements on a stage of indifferent quality. The objective is provided with an elastic mount. This permits a feeler-arm on the objective to glide in contact with an optically flat block of glass which is rigidly mounted with respect to the plate. Its plane surface is vertical and generally parallel to the track. Thus, measurements of the track position are made relative to the plane glass surface, and irregularities in the stage motion are demagnified by a large factor, roughly the magnifying power of the objective. Because the objective moves, it will accept the largest bundle of rays if the condenser aperture matches the N. A. of the lens and the source diaphragm is somewhat larger. A commercial version of this device is marketed by Leitz. The Leitz model UAM Ortholux microscope (see Fig. 8.12.3) is fitted with a stage for holding large plates. The optical flat, which is 150μ in length, contains a scale which is observed in the same field as the track. It enables one to read out the x position and lay out cell lengths very conveniently. A special condenser and objective for rotating the plate, as well as a Klausen type eyepiece micrometer, are also supplied as auxillary equipment.

A means for advancing the stage through any programmed schedule of cell lengths, or simply for advancing it by an accurately constant cell length is a feature of all good scattering microscopes. This may be accomplished, as in the Koristka MS-2, by a set of detents located so that the advance of the stage along the x axis encounters a sudden sharp resistance at each measurement station. Such stage displacements are typically $100\ \mu$.

Motor-driven stages are convenient. They may be stopped at the desired points by means of a punched tape, figured cam, or the like that operates the control switch.

The plate may be clamped on the stage mechanically, by vacuum, or if

mounted on an iron support, magnetically. The magnetizing current is usually a single pulse from a charged capacitor. The retentivity of the steel then holds the plate-mount firmly in position. To release the plate a demagnetizing current is adjusted so as to match the coercive force of the steel. A continuous current is not normally used to hold the plate. Direct current is most conveniently obtained from a rectifier, but the residual current ripple causes vibration.

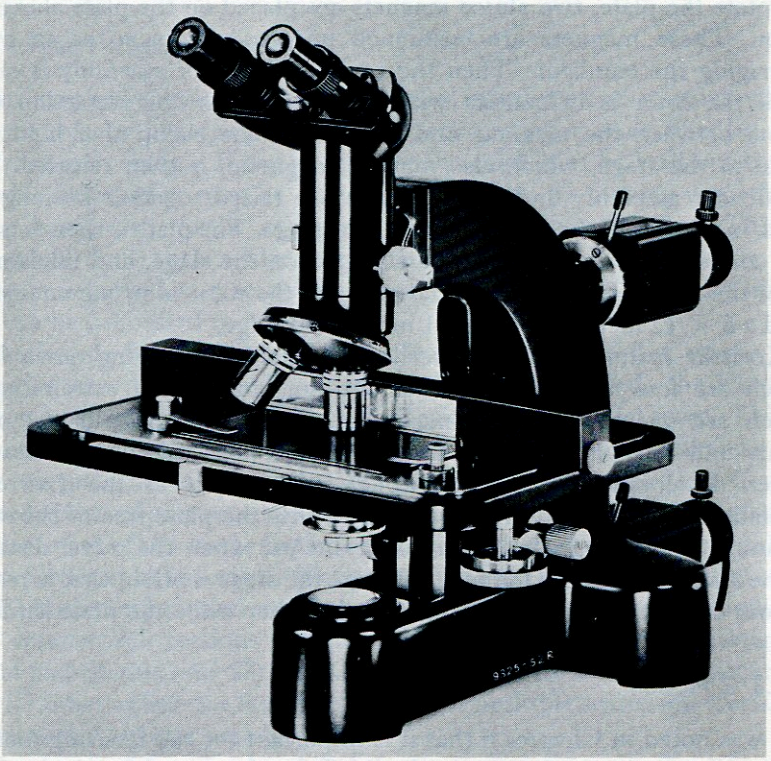

FIG. 8.12.3. Leitz microscope incorporating Stodiek principle for multiple scattering measurements. (Courtesy of E. Leitz.)

8.12.2 Plate Rotation

A means for rotating the plate about the optic axis of the microscope so as to align the track with the x axis is a necessary feature of a good scattering microscope. In the process one must not lose the track. This is accomplished by clamping the plate to a part that can rotate around the axis. Rotation of the whole stage around the optic axis is not satisfactory, because such a motion does not align the track with the line of the screw

displacement. The Koristka MS-2 microscope is designed so that the plate is held by vacuum to a structure, coaxial with the condenser, that raises under it and rotates while the track remains in view. An example of a magnetically clamped device is that of Dyson *et al.* (D-W 56). A steel rotor with a flat top on which the plate can rest surrounds the condenser and moves up and down with it. It rotates in ball bearing ways on a stator which is part of the condenser mounting. When it is desired to rotate the plate, two alnico magnets are placed on the plate above the rotor. These magnets are cushioned on the bottom so as to avoid damaging the emulsion. Then the condenser-rotator assembly is raised until the rotor is in contact with the plate. A strong attraction then exists between the magnets and the rotor. The clamp that holds the plate to the stage, which also may be magnetic, is then released. The condenser assembly and the objective are raised together keeping the track in view until the plate is clear of the stage. The plate is then rotated, the condenser lowered, the plate clamped on the stage, and unclamped from the rotor. The magnetic clamping on the rotor is strong enough to hold a 6 × 12 inch plate within 1 inch of any edge.

Koristka manufactures an overhead turntable, extending down from which are four legs adjustable in position, and at the extremities of which are vacuum cups or magnetic clamps. These hold the plate firmly and the whole rotates about the optic axis. Similar devices are under development for conventional microscopes at the Lawrence Radiation Laboratory. Any device which lifts the plate free of the stage without losing the track has an important use when the travel distance of the stage is limited. One may reiterate the stage motion, that is return it from one extremity of its motion to the other while the plate is lifted.

8.12.3 *Z* Motion

It was noted in Chapter 6 that it is important for the focusing motion of the objective lens to be accurately parallel to the axis of shrinkage of the emulsion. For scattering measurements it is necessary in addition that there be no coupling between this motion and rotations, especially about the x axis, nor with translations along the y axis. These contribute to the noise when the track is dipping in the emulsion and it is necessary to adjust the control knob to keep the track focused. The mere operation of mechanical focusing introduces objectionable vibration and displacements, so that some of the best microscopes have hydraulic focusing control with the control knob remote from the moving parts of the microscope. This also may offer exceedingly fine focusing control. When well made, such a system need not leak, or require "bleeding"

duplicated so faithfully the motion of the driving motor that they did not require this feature.

8.12.5 Vertical Scattering Deflections

Mabboux (M 53) measured the multiple scattering of tracks in the vertical plane. The measurement was made partially automatic in that vertical motion of the stage relative to the objective was measured by the change of electrical capacity between capacitor plates; the separation of the capacitor plates varied as the vertical distance was altered. This varied the frequency of an oscillator. The frequency was beat against a standard frequency, and by means of a frequency meter the variations of the capacitance were ultimately converted into galvanometer readings. The galvanometer deflection was calibrated by means of an interferometer to measure the z coordinate of the objective.

The vertical coordinate of a track, nevertheless, cannot be measured with the same accuracy as a lateral coordinate. The finite depth of focus, the emulsion shrinkage, and extra distortions are responsible. Typically a pellicle of nonuniform thickness is taken from a stack where neither surface is confined to a plane. When mounted on a (plane ?) surface of glass, very serious vertical displacements can occur. This effect is much reduced when glass-backed emulsions are exposed and processed.

8.12.6 Automatic Recording and Calculation

To obtain a good measure of the multiple scattering, one may wish to calculate third or higher differences in addition to the second. He also may decide to eliminate noise by any one or more of a half-dozen of the schemes outlined in Section 8.9. For these reasons a flexible automatic calculation procedure has been adopted by the writer's group in the Lawrence Radiation Laboratory. Primary data in the form of the coordinates $y_0, y_1, \cdots, y_n$ are read out on IBM cards and the scattering is calculated by an IBM 650 data processing machine according to any program supplied. The program normally used cuts off large second differences in the standard way. It has been objected that one does not obtain with this system an immediate answer, since the microscope is not connected directly to a calculator. The results are in some ways more objective, however, and this system leads to orderly procedures for data processing and very great flexibility. Of course, if a strange result is found, the scattering measurement usually can be repeated, and sometimes repetition of all measurements by another observer is routine.

The equipment used consists of a Koristka MS-2 microscope altered as follows: To allow the use of large plates, the yoke has been length-

ened. Any track on a plate 30 cm square can be rotated and scattered. The filar micrometer eyepiece is directly coupled to a Datex Corporation encoder made up of two units C713 and C714. The least read is 0.0013 μ. The hairline screw and the encoder turn as a unit. The rotation is brought about by stretched wires wrapped around a pulley that turns the screw. The rotation of a knob located low on the right side of instrument is transmitted to the pulley via the wires.

Many other devices have been developed for reducing the labor of multiple scattering measurements and calculations. For example, V. Brisson-Fouche (B 59.3) has built an analog calculating device for computing directly the second differences. To the filar micrometer screw she attached a voltage-dividing potentiometer in such a way that its voltage output is proportional to the displacement of the cross hair. By rotating the potentiometer body relative to the filar micrometer screw, the voltage output can be returned to zero after each displacement. Then the first differences are generated directly. These voltages are stored in capacitors by an ingenious switching arrangement, and second differences are converted into voltage differences between capacitors that were charged successively. These differences are amplified and each is converted into a number of pulses proportional to the absolute second difference by electronic circuitry. The total number of pulses and the number of cells are counted by standard pulse counters, and from them is obtained the mean second difference. By further circuitry the mean second difference for cells of double length is found. Cut off is applied by inspecting the track for sharp scattering deflections prior to measurement. These points are excluded from the measured segments of track. With this device 100 cells can be measured and calculated in 8 min.

Stiller and Louckes (SL 56) employed a small variable transformer in place of a potentiometer to obtain a signal varying with the rotation of the filar micrometer screw. A servo motor then, by means of a cam, adjusts a balancing transformer of similar construction until there is no net output. The amount of adjustment required is converted into units of displacement by a digital converter and the result is printed on a tape.

Other methods for making automatic calculations have been described in numerous publications. Sanna (S 59.1), Belovitsky *et al.* (BKSC 58), Rüfenacht *et al.* (RWGL 58), Barkas (B 58.2), and Castagnoli *et al.* (CFM 58) describe typical equipment.

8.12.7 Lead Screws

Translation of the stage is normally brought about by lead screws, the quality of which largely determines the accuracy of many measurements.

Ten threads per centimeter is a standard pitch. This should normally be accurate to better than a part in 1000. Setting the stage position to a micron or better is a requirement for such a screw. The diameter of the screw is important. The largest diameter should be used that is compatible with over-all weight, size, and cost limitations of the stage. The rigidity of the screw increases rapidly with its diameter. Periodic errors that arise from bent screws are therefore reduced, and the area of contact on each thread increases with the screw diameter. Very good screws are 20-25 mm in diameter, and screws of less than 10 mm are unsatisfactory because of flexing and warping during fabrication. Standard scanning stages at the Lawrence Radiation Laboratory now have 12-mm screws. A 60° metric thread form is standard, although a square thread may have some advantages. Typical lead-screw specifications for a scanning microscope are given by Hodges (H 60).

Cutting of the threads may be done either on a lathe or by special thread-grinding equipment. When done on a lathe the material cannot be so hard as when ground. It is usually limited to a Brinnel hardness of 30. The screws are more prone to wear and bending than the hardened and ground screws. Metric thread cutting is difficult with most American lathes. On the other hand, lathe cutting produces less distortions of the metal from release of local stresses in the metal blank or by introduction of new ones. It is also easier to match internal and external threads to each other when they are fabricated on the same lathe setup. Commercial thread grinders in America are reluctant to guarantee metric threads, as often their equipment suffers from the same conversion problems as do lathes. Ground threads may suffer from the defect that the thread and bearing surfaces of the screw are not concentric, and this concentricity must be rigidly specified. By mounting a close fitting drive nut on the lead screw and turning the screw in its bearings, the wabble of the nut can be measured, and the specification checked.

In order to obtain drive nuts that fit ground screws, they should be made with taps that are ground on the same machines as those used for grinding the lead screws. The surface of a good lead screw should be finished to 4×10^{-6} inches or better, and be of 60-64 Rockwell hardness. The final processing of a lead screw is the lapping. Lapping can be used to correct roundness of lathe-cut threads, variations of lead and in pitch, and thread "drunkenness." Variation of pitch diameter is harder to eliminate and little success can be expected with screws of small diameter-to-length ratio owing to their flexibility.

Some excellent results in lead-screw manufacture have been obtained by lathe-cutting threads leaving only a minimum of material for cleanup. The screws were then hardened to 60 Rockwell thickness and finish

ground. Extensive lapping will develop a new axis for the threaded portion of the screw. This means that the bearing lands must be lapped to be concentric with this axis.

Hodges (H 60) suggests the following lapping procedure: a long nut of a soft material and at least one-third the length of the thread is split lengthwise and provided with spring tightening. The screw is turned around a vertical axis so that the nut moves vertically, up and down, as the screw is turned one way and the other. It is prevented from rotation, but its weight is counterbalanced, and it is otherwise free. Lapping compounds of graded fineness are used. They must be of types that break down with wear to permit flushing them out of the finished threads. A few hours of lapping a day is extended over several weeks while the nut ends are reversed and perhaps several nuts worn out. Procedures developed for the manufacture of ruling engine screws (S51.2, BB51, S34, S34.1, S37, S37.1) are recommended for microscope stage screws.

Depending on the stage design the lead screw either may advance as it turns, as in a micrometer, or merely advance a nut that is constrained not to turn. The micrometer-type drive is not useful for large stage displacements, but is satisfactory for an inch or two of motion.

The drive-nut type should be mounted in good bearings and end play eliminated. Precise alignment, which is facilitated by adjustable bearing blocks, is essential.

8.13 Special Measurement Methods

It happens in almost every study that some tracks are too steep for conventional scattering measurements; especially if the emulsion is distorted. Estimates of $p\beta/z$ often still can be made by application of the theory to the track measurements that are possible under the prevailing circumstances.

When a grid has been printed on each pellicle of a stack it often is a very reliable frame of reference. Then using the track segments in the pellicles for cells, the angles of the track with respect to the grid lines at the points where the tracks enter the pellicle may be usable data, as are the coordinates relative to the grid (B-M 57).

Aside from the shrinkage, the distortion of the surface layer of emulsion is normally severe only near the edge of the pellicle. The dip angle, when measured near the surface, is especially free from distortion effects, which are primarily laminar shears. One can measure angles of dip as a track enters the surface of successive pellicles, and with the

average path in the pellicles as a cell length, obtain a good estimate of the particle $p\beta/z$. Double length cells can be used for noise elimination in cases when the particle has traversed many pellicles.

If the track is dipping with an angle δ, then the cell length is $t \sec \delta$ when the projected cell is t. The observed sagitta will be increased by $\sec^{3/2} \delta$, while the rate of energy loss will be greater by the factor $\sec \delta$.

In general, the information derived from scattering measurements on a track can be increased by measuring the z coordinates of the particle trajectory in addition to the y coordinates. This also has the advantage that shear-type distortions which affect the y coordinates are largely eliminated. It requires, however, that the depth of focus be very small. Little is known regarding the noise that must be present because of inhomogeneity in shrinkage, and for the reasons mentioned above.

8.14 Statistical Geometry of Tracks

Insofar as a track can be considered a one-dimensional continuous and differentiable locus, the various definitions introduced in the differential geometry of space curves apply to it. In addition, it is possible to introduce some new integral concepts. Mere counting of some distinctive track features is possible, suggesting simple measurement procedures. Examples follow of feasible special measurements:

8.14.1 Grain Coordinate Distribution

The whole scattering information-content of a track is to be found in the coordinates of the centers of the track grains. No one has as yet made full use of this information, but Olsen, Wergeland, and Overas (OWO 55) have given a theorem applicable here. Given a track chord of length t extending along the x axis between $x = 0$ and $x = t$, they have proved the following:

The probability that at abscissa x, the track ordinate y will lie between y and $y + dy$ is

$$W(y)\,dy = \left(\frac{3}{2\pi\langle\phi^2\rangle\, x^2(1 - x/t)^2}\right)^{1/2} \exp\left[-\frac{3y^2}{2\langle\phi^2\rangle\, x^2(1 - x/t)^2}\right] dy \qquad (8.14.1)$$

for $0 < x < t$, where $\langle\phi^2\rangle$ $(= N\sigma\langle\omega^2\rangle t)$ is the mean square projected scattering angle between tangents at points separated by distance t. The derivation of Eq. (8.14.1) by the methods of this chapter is a suitable exercise for the reader.

For the actual projected distribution of grain centers, the variance

$(\pi D_0^2)/12$, where D_0 is the reading and grain-noise sagitta, must be added to the variance of y derived from this distribution function. With it, the measured (x, y) coordinates of all the grain centers in a segment of track can be used for a maximum likelihood calculation of $\langle \phi^2 \rangle$.

8.14.2 The Transverse Range

Consider the terminal portion, length R, of a particle track. Let it be placed so that the first and last grains of the track are on the x axis. Then let the ordinates, y_i, of the successive ordinate maxima and minima be measured. We define the *transverse range*, R_T, to be

$$R_T = |y_1| + |y_2 - y_1| + \cdots |y_i - y_{i-1}| + \cdots |y_n - y_{n-1}| + |y_n| \quad (8.14.2)$$

Here y_1 is the first maximum or minimum, y_n the last, and (y_i, y_{i+1}) is an adjacent maximum-minimum pair. Maxima and minima, of course, alternate in accord with Rolle's theorem. A few measurements have indicated that the mean value of R_T is about $0.05R$ for protons, and about $0.1R$ for pions. Unfortunately individual track measurements fluctuate enough so that pion and proton tracks are not completely resolved even for ranges of 2 or 3 mm.

8.14.3 The Integral Scattering

Between each maximum-minimum pair there is a point of inflection. Here the track has a slope $dy/dx = \tan \phi_i$. Suppose one measures the successive angles ϕ_i at these points. We define

$$\Phi = |\phi_2 - \phi_1| + |\phi_3 - \phi_2| + \cdots + |\phi_{n-1} - \phi_{n-2}| \quad (8.14.3)$$

This is the *integral scattering*. It is a function of the residual range that depends on the particle producing the track.

The particle whose tracks are seen in emulsion have wavelengths much smaller than the grain diameters in the track. Then a classical description of the path is sensible. The particle trajectory mathematically is very complex, consisting as it does of relatively straight segments alternating with segments in which the path has a small radius of curvature. The *track* is further complicated because it defines the particle path only by the occasional silver grains that develop generally along the particle trajectory, but which are not centered on it. These circumstances make a definition of a minimum scattering displacement necessary, or at least convenient. One may be assured that Φ and R_T as defined above are always convergent because the number of scattering

centers along the track is finite, but in practice one avoids ambiguity by introducing a minimum separation, $|y_i - y_{i-1}|_{\min}$, between a maximum-minimum pair. This must be exceeded for it to be counted in R_T and for the intervening inflection angle to be measured. This minimum might be about a micron or it can be adjusted in proportion to the grain size.

8.14.4 Inflection Density

The density of inflection points, as defined above, and the number of such points in a residual range R are measurable track features that may help to identify a track or to measure its scattering rigidity. The distance between successive points of inflection defines a length, the mean value of which is associated with a given particle and its velocity. The integral scattering is likewise a quantity which is determined by the particle mass, charge, and velocity. The ratio of the integral scattering to the path length contains most of the scattering information in that track segment.

8.14.5 Lateral Displacement

A particle in motion defines instantaneously a direction that can be extended indefinitely as a straight line. When the particle ultimately comes to rest in matter, owing to scattering it will be found displaced from a line drawn tangent to the track at any particular residual range by a distance that is a random variable. This average absolute distance increases as the initial velocity at which the line was defined increases, and it also varies with the particle mass and charge. The displacement is an easily measured quantity. For muons produced by the decay of pions at rest, which have a range of 602 μ, the mean absolute projected lateral displacement is about 70 μ. The standard deviation of the projected lateral deflection, moreover, is about 89 μ. These quantities are as characteristic of pion decay in emulsion as the muon range itself.

8.14.6 Track Crookedness

In addition to the natural quantities suggested above, one can also measure the scattering in other ways. For example, suppose the eyepiece focal plane contains two parallel lines of a standard length separated by a standard distance. Some segments of a particle track can be completely contained between these lines and some cannot. As one moves this instrument along the track through a distance R from its terminus, it will traverse portions of the track where the track axis cannot be contained

entirely between the lines. The fraction of a given track which cannot be contained between such lines we may call the track *crookedness*.

8.14.7 Residual Cells

Another similar function can be defined by limiting angles. Suppose on the eyepiece reticle there are three diametral lines, a central one and others making angles $\pm \Delta\phi$ with it. Then a measurement procedure is as follows: the central line is placed tangent to the track. Then one moves along the track without rotating the eyepiece until one of the other two lines is for the first time tangent to the track. The distance traversed is a cell. At this point the eyepiece is rotated until the central line is again tangent to the track and another cell is traversed. A cell, of course, terminates where a sharp deflection occurs and the new initial direction is determined by the direction of the track just beyond the scatter point. The cell, here defined, is the interval of track length in which the particle changes its projected direction of motion by the preassigned angle.

When the particle is about to come to rest, there is a number of *residual* cells in the residual range that increases with increasing scattering of the particle. The number of such cells, of course, increases monotonically with the residual range.

The density of cells in a track segment is a measure of the mass, charge, and velocity of the particle. It should be noticed, however, that we have eliminated *measurement* in favor of *counting* both in this definition and in the definition of the natural cell. One measures only the total track length. He then *counts* the cells to obtain the cell density or mean cell length.

All the above definitions and discussion can be applied to the independent scattering deflections in the vertical plane.

8.15 Track to Track Scattering Measurements

To aid in the elimination of distortion, stage noise, and emulsion dislocation effects, it is sometimes possible to make multiple scattering measurements between two nearly parallel tracks. If these are tracks of particles having the same $p\beta/z$, as they may be if they are from an accelerator beam, or are disintegration products of a heavy cosmic ray nucleus, then the mean square second-difference signal will be double that of a single track measured conventionally. The method must be applied with great caution when the tracks are displaced vertically from each other, for then serious distortion and dislocation effects may intrude. It is stated that good relative scattering measurements require that

separation in depth remain less than about 50 μ (BPM 57). In track to track scattering measurements, cells of several centimeters length have been used. See (LFS 50, GM 51, Y 54, KK 55), and (S 55.1) for some measurements by this method.

When an electron pair produced by a high-energy photon is measured in this way, only a lower limit for the energy of the pair can be derived. Then the observed second difference of the spacing between the tracks S_{12}^2 is the sum of the mean square scattering sagittas of the electrons: $S_{12}^2 = D_1^2 + D_2^2$. In Chapter 5 (see Volume II), the distribution of energy between the members of the pair is given.

When more than two tracks in the same general direction remain present in successive fields of view, it is possible to measure the scattering sagitta of each track for then

$$S_{ij}^2 = D_i^2 + D_j^2 \quad \text{and} \quad D_i^2 = (S_{ij}^2 + S_{ik}^2 - S_{jk}^2)/2 \tag{8.15.1}$$

When n tracks are present, $n(n-1)/2$ independent equations can be written.

8.16 Uncertainty in Direction of Particle Motion

Measurements made on its track can provide information on the initial direction of a particle's motion only within certain limits of error. The angles always are affected by distortion and uncertainty of the shrinkage factor, which are topics treated in Chapter 6. The instrumental and grain noise, together with the particle scattering, impose further limitations on the accuracy of measurement.

In the horizontal plane suppose the angle ϕ of the tangent at a fiducial point P_0 of the track has the value ϕ_0, and this is the quantity to be measured. Then, because of scattering, at a point P_1 on the track, removed a distance t, the angle will be ϕ_1. According to Eq. (8.4.3) $\langle(\phi_1 - \phi_0)^2\rangle = N\sigma\langle\omega^2\rangle t$. The mean square angle between the tangent at P_0 and the chord connecting P_0 and P_1 is one-third of this. There is an additional variance term amounting to $(2\langle\delta^2\rangle/t^2)$ (or less) that arises from errors in the estimation of the position of the particle trajectory at the two ends of the chord. The total variance σ_ϕ^2 then is:

$$\sigma_\phi^2 = \frac{1}{3} N\sigma\langle\omega^2\rangle\, t + \frac{2\langle\delta^2\rangle}{t^2} \tag{8.16.1}$$

This is minimum when

$$t^3 = \frac{12\langle\delta^2\rangle}{N\sigma\langle\omega^2\rangle} \tag{8.16.2}$$

Now the noise level, D_0, in measing D_t is $(12/\pi\langle\delta^2\rangle)^{1/2}$, so that $12\langle\delta^2\rangle = \pi D_0^2$. On introducing $D_t^2/t^3 = (4N\sigma\langle\omega^2\rangle)/3\pi$, the condition for minimum error is that the cell t be chosen so that the scattering sagitta D_t is related to D_0 by:

$$D_t = \sqrt{\frac{4}{3}}\, D_0 \tag{8.16.3}$$

We set $K_c \approx 25$ (for distances in microns and p in Mev/c). Then the optimum track segment is

$$t_{\text{opt}} \approx 9\left(\frac{p\beta D_0}{z}\right)^{2/3} \tag{8.16.4}$$

This formula agrees with that of Inman (I 57) but differs from one derived using a result of Dilworth *et al.* (DGGL 50), who state that the noise effect is proportional to $t^{-3/2}$.

Actually the rule, Eq. (8.16.4), for the length of track segment to use in a measurement is only a general guide. If a length t_{opt} puts the point P_1 beyond where the track direction detectably changes, it would not be sensible to measure beyond the point of deflection. On the other hand, if no change in direction is detectable in the track segment one, may quite properly use a segment exceeding the length, t_{opt}. The meaning of t_{opt} is that it is the segment length at which one would typically first be able to detect a deviation from the initial track direction.

Using the length, t_{opt}, one can calculate σ_ϕ^2 from Eq. (8.16.1).

$$\phi_\phi^2 = 0.02 D_0^{2/3}\left(\frac{z}{p\beta}\right)^{4/3} (\text{radian})^2 \tag{8.16.5}$$

Thus, for example, with $p\beta/z = 100$ Mev/c and a noise level of 0.15 μ, it should generally be possible to determine ϕ_0 with an error of not much more than a fifth of a degree when distortion is not present. The accuracy with which the initial dip angle can be measured is not this good. The same analysis applies as that given for ϕ, but the additional noise of the finite depth of focus of the microscope must be added. In addition, vertical dimensions are reduced by the shrinkage factor, in which a systematic error also generally exists.

An empirical estimate of the error in the measurement of either a dip or azimuth angle can be made if the particle velocity does not change appreciably in the portion of the track used for the following measurements: suppose the track is divided into n segments each of length t. The average direction of the ith segment is observed to be α_i and $\langle(\alpha_{i+1} - \alpha_i)^2\rangle$ is the observed mean square charge in direction in going

Furth (F 55), and Kim (K 58.2). Their results are somewhat divergent in the details. The following discussion will not examine all the subtle points, but merely seeks to obtain a good measurement of the particle momentum as simply as possible.

Let n angles ϕ_i be measured in projection between successive tangents to a track at points spaced by a distance t. If the track has a dip angle, δ, these points are actually separated by a distance t sec δ. In the presence of a magnetic field H along the line of sight, the average value of the ϕ_i is given by

$$\langle | \phi | \rangle = \frac{3 \times 10^{-4}\, z(H \sec \delta)\, t}{p} \tag{8.17.1}$$

The scattering produces a variance, S^2, in the distribution of the ϕ_i and the magnetic bending may not exceed S unless the field is high. The scattering, however, is itself an additional source of information. The quantity S^2 is equal to

$$\frac{1}{n}\left(\sum_1^n \phi_i^2\right) - \left(\frac{1}{n}\sum \phi_i\right)^2 = \frac{K_c'^2\, z^2 t \sec^3 \delta}{p^2\beta^2} + S_n^2 \tag{8.17.2}$$

where S_n^2 is a noise term that is independent of t, H, or δ. The noise can be evaluated by varying the cell size in the usual manner. The expressions (8.17.1) and (8.17.2) are independent. With knowledge of the particle mass, the weighted average of these momentum estimates is more reliable than either alone. On the other hand, the particle mass is determined by the measurements if one chooses to use the equations in that way.

In a field of 300,000 gausses, Furth (F 55) shows that one centimeter of track yields as much information as is obtainable by scattering alone from a segment 9.2 cm in length. If the scattering information were neglected, the effective track length would be 8.2 cm. On the other hand, when the field is 100,000 gausses, use of the scattering information in addition to the magnetic bending gives a gain factor in effective track length of 2.3.

Scattering information is optimized if the cell length t is about that yielding the maximum information in the absence of the magnetic field.

Currently there is much interest in using emulsion in strong magnetic fields. For example, development of excellent magnets at CERN has been carried out for this purpose (G 61).

Birdsall and Furth (BF 59) have developed a successful magnet for subjecting emulsion to fields of 200,000 gausses or more. Its general appearance is shown in Fig. 8.17.1. The magnet windings, following a design due to Bitter (B 39.1), are circular disks of Berylco 10. In the center of each, a 2-inch hole has been made. The disks are 0.045 inches

in thickness and are insulated from each other by resin-bonded Fiberglas sheets. Each disk is slit radially, and the ends soldered to the two neighboring disks so as to form a helix. Heavier end disks carry current in and out. The whole assembly is tightly clamped together because eddy currents, particularly in the end pieces, produce large transient repulsive forces.

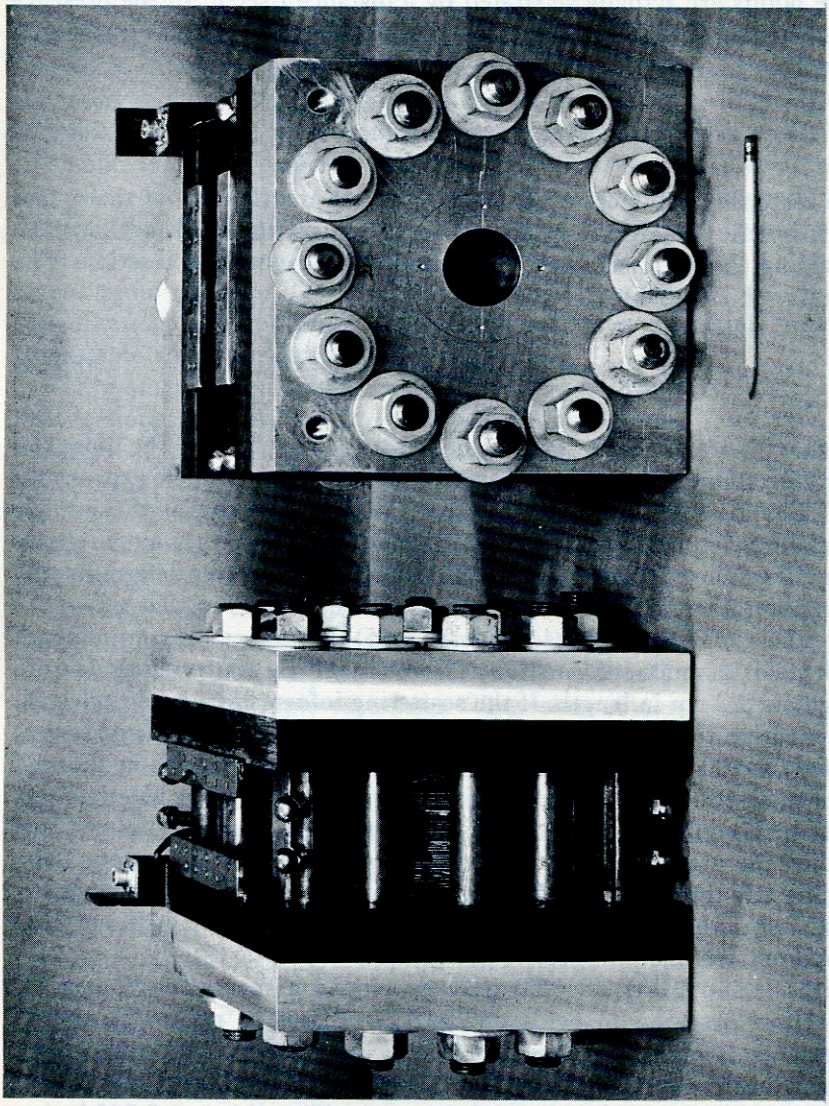

FIG. 8.17.1. Birdsall and Furth magnet (IDLRL).

The power supply consists of a 750 microfarad capacitor bank charged to 13.5 kv. The rise time is 250 microseconds, and a field that remains constant to 1% can be maintained for 50 microseconds. The current is 55,000 amperes. A pulse rate of 11 per minute has been used. The pulse is initiated by two 5555 ignitrons in parallel. Four other ignitrons are used for short-circuiting the magnet through stainless-steel resistors. The magnet is cooled by a thin tubular stream of silicone oil between the emulsion, which is on the axis of the solenoid, and the copper disks. The oil is chilled to dry-ice temperature and cools the coil at its inside surface. Care must be taken that water condensation on the cold surfaces does no damage, and the silicone oil itself must be free of water.

A stack of 120, 600 μ emulsion pellicles each in the form of a 2-inch circular disk can be inserted in the magnetic field. The field is perpendicular to the emulsion surfaces. The beam then also is most conveniently made parallel to the coil axis. At dry-ice temperature emulsion shrinks, and the stack should be constructed so that the pellicles will not become loose relative to their neighbors.

Since the length of time that the current can be held steady at the peak value is not large, the beam from an accelerator must be pulsed so that it reaches the emulsion only during the constant peak-field interval. With the Lawrence Radiation Laboratory Bevatron it has been possible to obtain 30 microsecond pulses of negative K mesons synchronized with the pulsed magnet. An improvement to this magnet has recently been made by vacuum impregnation of the assembly with epoxy resin. This reduces vibration and danger of plate-to-plate insulation failure. The magnet is now water-cooled. The potting procedure makes the bore watertight. Cooling is accomplished by passing a thin high-velocity water stream between the bore and a concentric lucite tube. This assembly has been operated at 300,000 gausses without damage, and in a life test 30,000 pulses at 200,000 gausses produced no evidence of deterioration.

The first important applications of this magnet have been made by R. S. White and his collaborators. It has been used for the determination of sign of charge and energy spectrum of pions produced in the capture of negative K mesons in emulsion. When the pion energy is above 60 Mev the magnetic field of 2×10^5 gausses determines the energy better than when it is measured by grain counting, and it also determines the sign of the pion without the labor of tracing the track to its terminus. The method used is simply to measure the change in direction, ϕ, for a cell of 1 cm. Sharp deflections of more than 3° in this segment of path are subtracted out, and the remainder are used to calculate $\langle \mid \phi \mid \rangle$. About one particle in three experiences a sharp deflection. Even the use of this

magnet, however, has not solved the important problem of negative hyperon identification, because in general the hyperon velocities and ranges are still too small for magnetic deflection measurements.

A magnet that produces a pulsed field of 120,000 gausses with an inside diameter of 2.5 cm has been used by Likhachev *et al.* (LKB 56) to measure electron-pair energies. The spectrum obtained agrees well with that measured by the multiple scattering.

An interfering effect that can be most serious for emulsion measurements of curvature is distortion. The behavior and the magnitude of the distortion vector must be established for reliable measurements to be made. No one seems as yet to have studied the effect of the correlation between successive scattering events that can occur when the particles are polarized. This could simulate the effect of magnetic bending.

The reduction of scattering obtainable in dilute emulsions suggests their use in magnetic deflection work. A reduction of 16% is anticipated by Dilworth and Goldsack (DG 53).

Ionization and Track Structure

9.1 Delta Rays in Emulsion

When a particle of charge ze and mass μ penetrates matter, its electric field disturbs the atomic electrons. These interactions constitute collisions of varying energy transfer in which the kinetic energy of the particle is dissipated.

If an electron in sensitive emulsion receives kinetic energy exceeding perhaps 2000 ev in such an encounter, its range may be sufficient for its track in emulsion to be seen projecting from the trajectory of the primary particle. Such electron tracks are known as delta rays.

The differential cross section for transfer of energy in the interval dw to a *stationary unbound* electron is calculable for the electric field of a point charge, ze (R 52). It is:

$$\left(\frac{d\sigma}{dw}\right) dw = \frac{2\pi z^2 r_0^2 mc^2}{\beta^2}\left(1 - \frac{\beta^2 w}{w_{\max}}\right)\frac{dw}{w^2}\ \text{cm}^2 \qquad (9.1.1)$$

Small terms which depend on the particle structure and the sign of the charge are neglected, and no allowance for the physical state of the matter traversed is made in this approximation.

The symbols in Eq. (9.1.1), which describes the differential delta-ray spectrum, are defined as follows: the particle velocity is βc, m is the electron mass, c is the velocity of light, $\gamma = (1 - \beta^2)^{-1/2}$, and $r_0 = e^2/(mc^2)$. The energy, w, of such knock-on electrons extends up to a maximum value:

$$w_{\max} = \frac{2mc^2\beta^2\gamma^2}{1 + 2\left(\frac{m}{\mu}\right)\gamma + \left(\frac{m}{\mu}\right)^2} \qquad (9.1.2)$$

The lower limit of w that defines a recognizable delta ray in emulsion depends on many things. These include the range-energy relation for low-velocity electrons, the grain size of the emulsion, the scattering of these slow electrons, the sensitivity of the emulsion, and the density

of background electron tracks. One must adopt certain conventions for counting delta rays. Some proposed by Tidman, George, and Herz (TGH 53) are judged to be practical. They have counted the number, ν, of delta rays produced per centimeter of track of a singly charged particle, as a function of its velocity for various conventions.

According to Eq. (9.1.1) the density of delta rays increases with the square of the particle charge, but in counting one must allow for the fact that the core of the track itself broadens as the particle charge increases, and the conventions may require adjustment for tracks of very heavy nuclei. For light nuclei we take the delta-ray density, n_δ, to be $z^2\nu$ when the velocity is high enough for the nucleus to be stripped of electrons. If a differential segment of the track has a length dR, then the total number of delta rays on a track between the point where the particle velocity is βc and the point where it comes to rest is

$$N_\delta = \int_0^R n_\delta \, dR \tag{9.1.3a}$$

When an element of proton path, $d\lambda$, encompasses the same velocity interval as the track element dR, $d\lambda = (z^{*2}/M)dR$, (see Section 9.4) where z^{*2} is the mean square effective charge for energy loss, and M is the particle mass in units of the proton. Also, in general, $n_\delta = z^{**2}\nu$, where z^{**2} is the mean square effective charge for production of delta rays. In general z^* and z^{**} will not be exactly equal.

Then we have:

$$N_\delta = \int_0^R n_\delta \, dR = M \int_0^\lambda \frac{z^{**2}}{z^{*2}} \nu \, d\lambda \tag{9.1.3b}$$

The ratio z^{**2}/z^{*2} is usually sufficiently near unity so that one can approximate, and write $N_\delta = M \int_0^\lambda \nu d\lambda = M\Delta(\lambda)$.

Table 9.1.1 for $\Delta(\lambda)$ has been prepared using a recommended convention of Tidman, George, and Herz. The convention chosen for G.5 emulsion was as follows.

Grain configurations, to be counted as delta rays, must attain a minimum displacement of 1.58 μ from the axis of the track as seen projected on the plane of the emulsion. In the vicinity of 1.58 μ the number of delta rays counted appears to vary inversely with the magnitude of the minimum displacement.

Other delta-ray conventions have been studied, and the definition of a delta ray by a certain minimum number of grains, say 4, has frequently been applied (DFK 52). In each case a correction is to be made for background. This can be evaluated well enough by recording

the number of apparent delta rays on proton tracks of residual range less than 100 μ where no true delta rays are expected.

Each set of conventions requires investigations as to its completeness and objectiveness, and each leads to a different table of delta-ray densities.

TABLE 9.1.1

THE DELTA-RAY DENSITY AND ITS INTEGRAL

λ(cm)	ν(cm^{-1})	$\Delta = \int \nu d\lambda$	λ(cm)	ν(cm^{-1})	$\Delta = \int \nu d\lambda$
100×10^{-4}	0	0.00	7	29	334
200	2	0.01	8	27	362
300	6	0.06	9	26	389
400	13	0.15	10	25	415
500	20	0.31	11	25	440
600	34	0.61	12	24	464
700	47	1.0	13	24	488
800	59	1.6	14	23	511
900	66	2.2	15	23	534
1000	72	2.9	20	21	644
1500	89	7.1	25	20	744
2000	97	12	30	19	841
2500	98	17	40	18	1026
3000	96	22	50	17	1201
3500	91	26	100	12	1926
4000	88	31	200	11	3076
4500	85	35	300	10	4126
5000	82	44	400	10	5126
6000	78	52	500	10	6126
7000	74	60	1000	9	10,876
8000	70	67	>1000	9	$10{,}876 + 9(\lambda - 1000)$
9000	67	74			
1×10^{0}	65	81			
2	59	139			
3	47	189			
4	41	233			
5	35	271			
6	31	304			

No final evaluation of the relative usefulness of different measures of the delta-ray density has been made. In Fig. 9.1.1 tracks at the minimum of ionization are shown that illustrate the effect of the particle charge on the structure of the track, and also illustrate the difficulty of obtaining objective delta-ray measurements. It is not surprising that observers differ in the counts they obtain. The problem of counting delta rays is complicated, also, by the emulsion sensitivity and grain size. The

number of delta rays observed will depend on the resolution of the emulsion and on the sensitivity. Fast delta rays tend to be missed in low-sensitivity emulsions. It is recommended that each observer be calibrated by counting a standard track, and that he frequently check his calibration. Each separate emulsion batch also probably requires calibration.

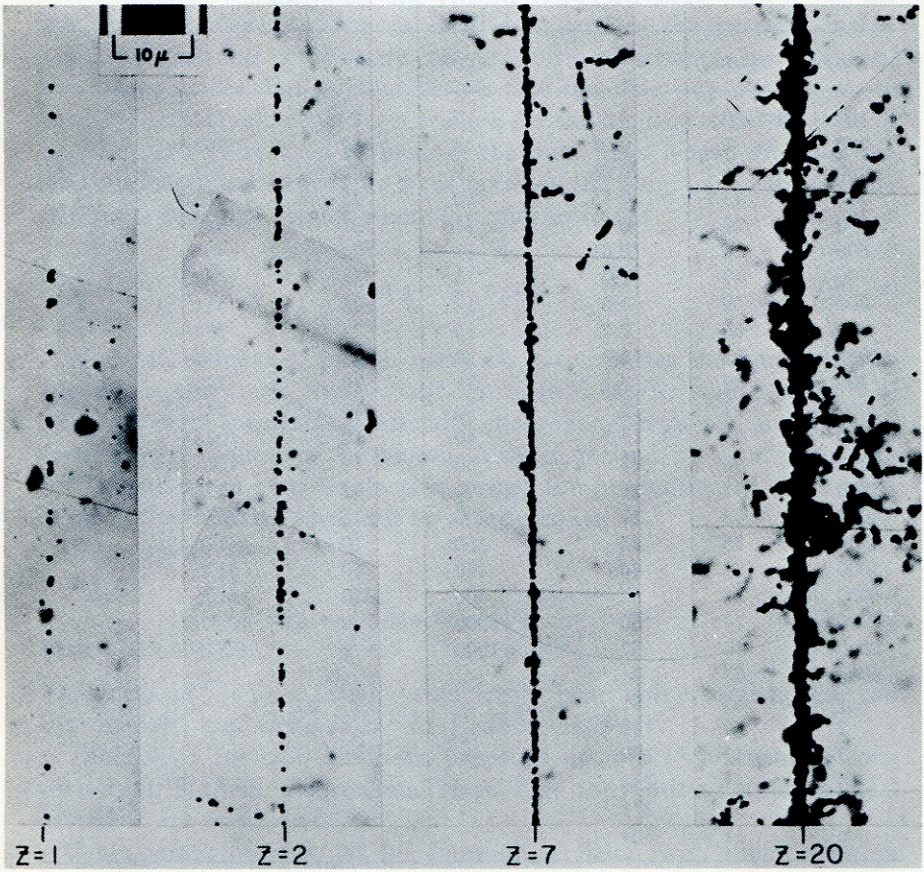

FIG. 9.1.1. Tracks of particles with $Z = 1, 2, 7$, and 20 at the minimum of ionization in G.5 emulsion. (Courtesy of M. M. Shapiro.)

Demers (D 58) has given results of extensive delta-ray counting in his special fine-grain emulsions, and he has evaluated the efficiency of counting under certain conditions. The "efficiency" was found sometimes to exceed 100 %. It is known that Eq. (9.1.1) fails for small

energy transfers. The selection criteria for delta rays also probably were not such that the minimum energy could be known accurately.

At relativistic velocities, when $\beta \to 1$, w_{max} becomes large compared to any practical minimum delta-ray energy, so from Eq. (9.1.1), the number of delta rays exceeding a particular minimum energy w_{min} becomes simply:

$$n_\delta \approx (2\pi r_0^2) \frac{mc^2}{w_{min}} z^2 = \text{constant} \times z^2 \qquad (9.1.4)$$

If the constant for the particular counting convention is determined empirically for particles of known charge, such as relativistic alpha particles, then the charge of other relativistic particles can be determined

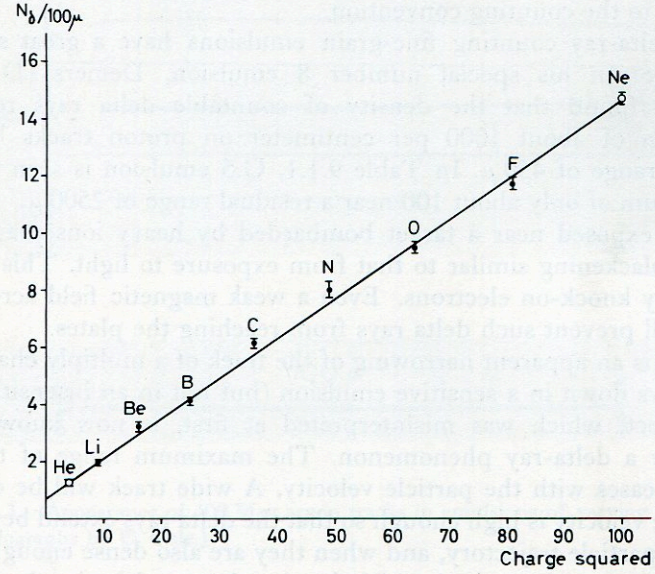

FIG. 9.1.2 Dependence of delta-ray number on the particle charge. (Courtesy of O. Mathiesson.)

with good accuracy. Mathiesson (M 60.1) counted as delta rays the grain configurations on relativistic tracks extending from the axis of the track by 1.3 μ or more, and plotted the density of such tracks as a function of z^2. The charge was determined by the photometer of von Friesen and Kristiansson (VK 52). In Fig. 9.1.2 the straight line resulting from his measurement is shown. Note that there is a finite intercept at $z = 0$.

Presumably this is the background that should be subtracted from all his readings. If a track is not relativistic, but a sufficiently long segment of it is available for measurement, the energy loss from the stopping theory (Section 9.4) may be combined with the approximate inverse square-dependence on the velocity of any measure of the delta-ray density to yield an estimate of the charge, ze.

By using the range-energy relations for heavy ions (Chapter 10) and Table 9.1.1, or its equivalent for other counting conventions, heavy ions coming to rest in emulsion also may be identified. The uncertainty of such an identification usually is such that one can equate M to $2z$.

In an early paper Hoang (H 51) applied the formula (9.1.1) to particles of low velocity with the then existing range-energy relations. He found with a particular counting convention that the delta-ray density varied as $z^{1.54}R^{-0.46}$, R being the residual range. These exponents should not be sensitive to the counting convention.

For delta-ray counting fine-grain emulsions have a great statistical advantage. In his special number 8 emulsion, Demers (D 58), for example, found that the density of countable delta rays reaches a maximum of about 1000 per centimeter on proton tracks having a residual range of 450 μ. In Table 9.1.1, G.5 emulsion is seen to attain a maximum of only about 100 near a residual range of 2500 μ.

Plates exposed near a target bombarded by heavy ions may receive surface blackening similar to that from exposure to light. This effect is caused by knock-on electrons. Even a weak magnetic field across their paths will prevent such delta rays from reaching the plates.

There is an apparent narrowing of the track of a multiply charged ion as it slows down in a sensitive emulsion (but not in an insensitive one). This effect, which was misinterpreted at first, is now known to be primarily a delta-ray phenomenon. The maximum range of the delta rays increases with the particle velocity. A wide track will be observed when the velocity is high enough so that the delta rays extend beyond the primary particle trajectory, and when they are also dense enough to give an appearance of continuity. Obviously, the emulsion grain size and sensitivity, as well as the amount of physical development, affects the appearance of the track.

In Fig. 9.1.3 one sees the tracks of 400 Mev argon ions in emulsions of several different sensitivities. The tapering of the track as it slows down is observable in the most sensitive emulsions, but in the least sensitive emulsion the ionization produced by the delta rays is not registered. In Fig. 9.1.4 photomicrographs of the tracks of several ions, all of the same initial velocity, are shown as they appear in G.5 emulsion. They all exhibit the tapering phenomenon, but it is less marked for the lighter ions.

There will always exist a residual range at which the solidly developed core of the track has a maximum width. This range is known as the *thin-down length*. For a particular sample of uniformly developed emulsion it is a function of the nuclear charge, but no universal meaning can be attached to it. For a very knowing investigator it may be a useful

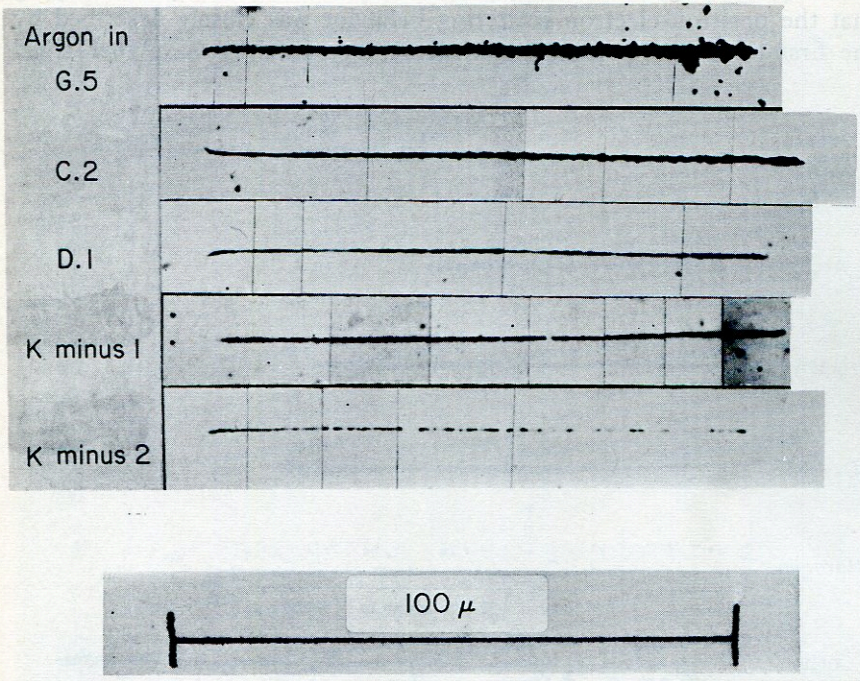

FIG. 9.1.3. Appearance of 400 Mev argon tracks in emulsions of varying sensitivity. (Photomicrographs by C. Cole.)

quantity, but generally only the following rule applies: at a given nuclear velocity and in a particular sample of uniformly developed electron-sensitive emulsion the track width rises monotonically with the atomic number of the nucleus, and approaches an asymptotic value determined by the maximum range of the delta rays. This maximum range does not depend on the nuclear charge but increases with the particle velocity.

Hoang (H 51) also observed that a certain measure of the track width varied in proportion to the square root of the residual range,

and the thin-down length was proportional to z, but in the writer's opinion such rules must be checked in each emulsion sample, and for each measure of the track width.

Electrons and positrons have delta-ray distributions that are slightly different from those of heavy particles. The differences are important only for rare collisions of large energy transfer, however, and Barkas, Deutsch, Gilbert, and Violet (BDGV 52) succeeded only in verifying that the positron-electron scattering behavior was closely described by the first term of Eq. (9.1.1). All elementary particles have theoretical

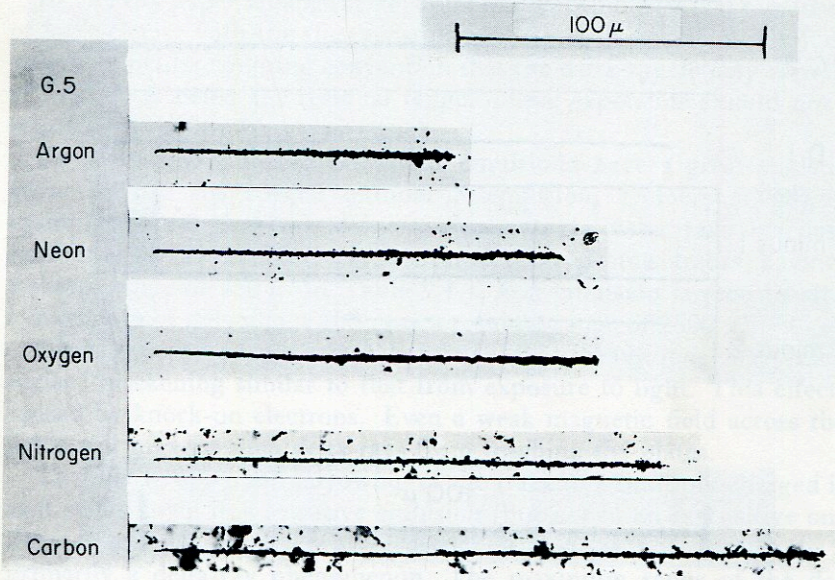

FIG. 9.1.4. Appearance of tracks in G.5 emulsion made by ions of varying atomic number, each of energy 10 Mev/nucleon. The tracks in each case taper as the ion velocity falls and less energetic delta rays can be produced. (Photomicrographs by C. Cole.)

delta-ray distributions (W 33) that depend on the particle spin and structure when the energy transfer is near w_{max}, but these differences have not been observable in emulsion studies.

Were it not for atomic binding effects, the energy, w, and angle of emission, θ, of delta rays from heavy particles would be directly connected by the relation: $w \approx w_{max} \cos^2\theta$; $\theta < \pi/2$. The electron binding and the scattering experienced by low-energy delta rays tends to make this a relationship of limited usefulness. However, there remains a forward-to-backward asymmetry in the emission of delta rays from a

track that can be invoked to determine the direction of motion of the particle (see Fig. 9.1.5).

Ekspong (E 57.1) found that between $\beta = 0.3$ and $\beta = 0.98$, and for $z = 1$ the fraction of delta rays projected into the forward hemisphere is 0.61 ± 0.01. The direction of the delta ray is taken to be the direction defined by the first two grains of the delta-ray track that are clearly not part of the primary track. This is not a function of the sign of the particle.

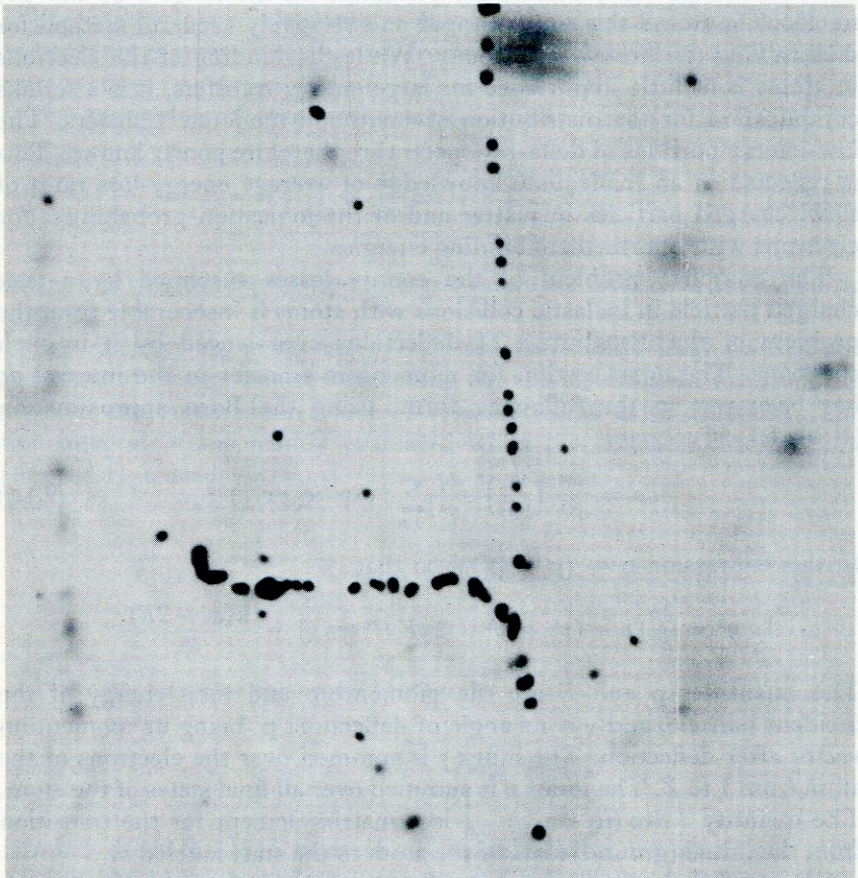

FIG. 9.1.5. Delta ray whose initial direction appears to indicate the direction of motion in the primary track. (Photomicrograph by G. Cole.)

No dependence on primary particle velocity was detected. It seems also not to depend on the number of grains in the delta-ray track for delta rays of three grains or more. (The number of delta rays with many grains is very small.) This result enables one to determine the direction of a track with 99% certainty if as much as 3 cm of track is available for study.

Hèbert (H 58.4) measured both the angle and the energy of the *fast* delta rays from heavy cosmic-ray primaries. In the range 3-50 Bev per nucleon, he found this to be a rapid and relatively accurate method for determining the heavy-ion velocity. While the binding of the electrons in atoms is of little importance for large energy transfers, it is a serious complication for the distribution of small and moderate transfers. The low-energy portions of delta-ray spectra are therefore poorly known. This is reflected in an inadequate knowledge of average energy-loss rates of slow, charged particles in matter and of the ionization probabilities for electrons with intermediate binding energies.

The complete problem of the energy losses sustained by a fast, charged particle in inelastic collisions with atoms is inseparable from the problem of the distribution of deflections experienced by it in such collisions. The cross section for momentum transfer in the interval dq has been put in the following form, using the Born approximation (B 30, LL 56):

$$d\sigma = \frac{8\pi}{\beta^2}\left(\frac{z}{137}\right)^2 \frac{dq}{q^3} \sum_{j,n} |\exp(i\mathbf{q}\cdot\mathbf{r}_{j,n})|^2_{0,n} \tag{9.1.5}$$

In this expression $\mathbf{q} = (\mathbf{p} - \mathbf{p}')/\hbar$ so that

$$q^2 = \frac{2p}{\hbar^2}[p - (p^2 + w^2 - 2wE)^{1/2}\cos\chi] + \frac{w(w-2E)}{\hbar^2}$$

The quantities $\mathbf{p}$ and E are the momentum and total energy of the incident particle, and χ is its angle of deflection, $\mathbf{p}'$ being its momentum vector after deflection. The index j is summed over the electrons of the atom from 1 to Z. The index n is summed over all final states of the atom. The quantity $|\exp(i\mathbf{q}\cdot\mathbf{r}_{j,n})|_{0,n}$ is a matrix element for the transition from the initial (ground) state of the atom to the state labeled n.

For small deflections of the incident particle in the field of an atom,

$$\hbar^2 q^2 = (w/v)^2 + p^2\chi^2 \tag{9.1.6}$$

The lower bound on q is therefore $w/(\hbar v)$, when energy w is transferred to an electron. An exact treatment of the distribution of energy losses is not possible without detailed atomic and molecular structure information, and we may not pursue this problem further here.

9.2 Energy Loss by Collision with Electrons

Charged particles lose some energy by elastic collisions with atomic nuclei or may be lost from a beam entirely in catastrophic interactions. Charged particles also radiate in the fields of atomic nuclei. As energy-loss processes, these are important compared to electron collisions only for high-energy electrons and for very slow or very fast heavy particles.

The energy loss to electrons in unit path suffered by a point charge penetrating matter is calculated from the differential energy-transfer cross section, $(d\sigma/dw)dw$ [Eqs. (9.1.1) and (9.1.5)].

The energy loss, $\mathscr{I}$, per centimeter is:

$$\mathscr{I} = n\int_{w_0}^{w_{\max}} w\frac{d\sigma}{dw}\,dw + n\int_{w_{\min}}^{w_0} w\frac{d\sigma}{dw}\,dw \tag{9.2.1}$$

where n is the number of electrons per cubic centimeter in the stopping material.

The quantity w_0 is an energy selected sufficiently large so that for collisions of energy transfer exceeding w_0, the electrons in the stopping material can be considered free. These are called close collisions. The first integral, $\mathscr{I}_1$, is readily evaluated when the collision cross section (Eq. 9.1.1) is used.

Then:

$$\mathscr{I}_1 = n\int_{w_0}^{w_{\max}} w\frac{d\sigma}{dw}\,dw = \frac{2\pi nz^2r_0^2mc^2}{\beta^2}\left[\ln\frac{w_{\max}}{w_0} - \beta^2\right] \tag{9.2.2}$$

$w_0 \ll w_{\max}$

The calculation of the second integral

$$\mathscr{I}_2 = n\int_{w_{\min}}^{w_0} w\frac{d\sigma}{dw}\,dw$$

is much more involved because all possible electronic transitions must be considered, and the detailed structure of the stopping material is important. The formula of Bethe (B 32) is now the most widely adopted estimate of the rate of energy loss of a fast particle in distant collisions. He gives:

$$\mathscr{I}_2 = \frac{2\pi nz^2r_0^2mc^2}{\beta^2}\left[\ln\left(\frac{2mc^2\beta^2\gamma^2w_0}{I^2}\right) - \beta^2\right] \tag{9.2.3}$$

The quantity I introduced in this calculation of the energy loss is known as the *mean ionization potential*, (also known as the mean excitation potential). For a range of high velocities, I is independent of the particle velocity. It depends on the atomic number, Z, of the stopping material.

It is defined in terms of the *oscillator strengths* f_α as follows: $\ln I = \Sigma f_\alpha \ln W_\alpha$. The transition probability from the initial state in which an electron exists to an excited state of relative energy W_α is governed by the oscillator strength $f_\alpha = (2mW_\alpha/\hbar^2) \mid x_\alpha \mid^2$.

The matrix element $\mid x_\alpha \mid$ is calculated for the electron coordinate x between the two states in question. The set of final states extends into the continuum. These calculations are difficult and have not been done exactly. A compendium of oscillator strengths calculated on the hydrogenlike approximation has been prepared by Lewis (L 53.2). For heavy atoms F. Bloch (B 33 B 33.1) found that the ratio I/Z is about 1 Rydberg. At present I cannot be obtained with sufficient accurary from theoretical considerations alone, and one must resort to a semi-empirical evaluation of it. For a composite material such as emulsion, I is defined by:

$$n \ln I = \sum N_i Z_i \ln I_i \tag{9.2.4}$$

where N_i is the density of atoms of atomic number Z_i and mean ionization potential I_i in the composite material. Except at low velocities the stopping effects of the various atoms are nearly additive.

The sum $\mathscr{I} = \mathscr{I}_1 + \mathscr{I}_2$ is the total energy-loss rate to electrons. Adding Eqs. (9.2.2) and (9.2.3) one obtains:

$$\mathscr{I} = \frac{2\pi n z^2 r_0^2}{\beta^2} \left[\ln \frac{2mc^2\beta^2\gamma^2 w_{\max}}{I^2} - 2\beta^2\right] mc^2/\text{cm} \tag{9.2.5}$$

This expression well describes the energy loss in the interval where the particle velocity is large compared to the velocity of the fastest electrons of the stopping material, but not extremely relativistic. When the energy is very high, the rise of ionization beyond the minimum implied by Eq. (9.2.5) is restricted in condensed materials by the polarizability of the stopping medium. At the lower limit of validity of Eq. (9.2.5) the tightly bound electrons are perturbed only adiabatically by the slow moving particle, and do not contribute to the stopping. The logarithm then does not express this behavior correctly.

At both low and high velocities, therefore, a correction must be added to Eq. (9.2.3), and we take as an exact expression:

$$\mathscr{I}_2 = \frac{2\pi n z^2 r_0^2 mc^2}{\beta^2} \left[\ln \left(\frac{2mc^2\beta^2\gamma^2 w_{\max}}{I^2}\right) - 2\beta^2 - 2C\right] \tag{9.2.6}$$

Then we write for the rate of energy loss of a singly charged heavy particle:

$$\iota = \mathscr{I}/z^2 = \frac{2\pi n r_0^2 mc^2}{\beta^2}\left[\ln\left(\frac{2mc^2\beta^2\gamma^2 w_{\max}}{I^2}\right) - 2\beta^2 - 2C\right] \qquad (9.2.7)$$

A fairly reliable estimate of the correction term for standard emulsion can be made for protons above about 40 Mev (B 58.3). This has been done using the theories of Walske (W 56) and Sternheimer (S 56.1), applied respectively to the low-velocity and high-velocity regions. The value of C found in this way is given in Table 9.2.1. The corrections are not carried below 40 Mev because Walske's calculations are limited to the K- and L-shells, and at low velocities it is certain that corrections must also be made for higher shells (B 61.1). The mean ionization potential, I,

TABLE 9.2.1[a]

THE CORRECTION TERM C FOR STANDARD EMULSION

τ	C
40.0	0.055
50.0	0.048
70.0	0.038
100.0	0.030
140.0	0.023
200.0	0.016
260.0	0.011
300	0.009
400	0.006
500	0.005
700	0.004
1000	0.002
1200	0.004
1400	0.009
1600	0.020
1800	0.033
2000	0.046
3000	0.115
4000	0.184
5000	0.250
10,000	0.524
20,000	0.902
30,000	1.167

[a] The value of C is given as a function of τ, the kinetic energy of a proton of velocity βc. For a particle of mass M in units of the proton and kinetic energy T(Mev), $\tau = T/M$.

TABLE 9.2.2

THE ENERGY-LOSS RATE FOR PROTONS IN STANDARD EMULSION[a,b]

τ	ι	i	τ	ι	i
0.1	1500	394	8.0	124	32.5
0.2	1130	297	8.2	122	32.0
0.3	950	250	8.4	120	31.4
0.4	820	216	8.6	118	30.9
0.5	721	190	8.8	116	30.4
0.6	650	171	9.0	114	29.8
0.7	597	157	9.2	112	29.3
0.8	559	147	9.4	110	28.8
0.9	519	136	9.6	108	28.3
1.0	490	129	9.8	107	27.9
1.2	438	116	10.0	105	27.5
1.4	398	105	11	97.7	25.7
1.6	368	96.6	12	91.5	24.0
1.8	342	89.6	13	86.1	22.6
2.0	320	83.9	14	81.5	21.4
2.2	299	78.5	15	77.3	20.3
2.4	280	73.5	16	73.6	19.32
2.6	263	69.1	17	70.2	18.43
2.8	251	65.9	18	67.2	17.65
3.0	242	63.5	19	64.4	16.90
3.2	233	61.1	20	61.9	16.27
3.4	224	58.8	22	57.5	15.10
3.6	215	56.4	24	53.5	14.05
3.8	207	54.3	26	50.4	13.23
4.0	200	52.5	28	47.6	12.50
4.2	194	50.9	30	45.2	11.88
4.4	188	49.3	32	43.0	11.30
4.6	182	47.8	34	41.1	10.80
4.8	177	46.5	36	39.3	10.32
5.0	172	45.1	38	37.7	9.89
5.2	167	43.8	40	36.3	9.53
5.4	163	42.7	42	35.0	9.19
5.6	159	41.6	44	33.8	8.87
5.8	155	40.7	46	32.6	8.56
6.0	152	39.8	48	31.6	8.30
6.2	149	39.0	50	30.7	8.06
6.4	146	38.1	52	29.8	7.83
6.6	142	37.2	54	28.9	7.59
6.8	139	36.4	56	28.1	7.38
7.0	136	35.6	58	27.4	7.20
7.2	133	34.8	60	26.7	7.01
7.4	131	34.1	62	26.1	6.85
7.6	128	33.5	64	25.5	6.69
7.8	126	33.0	66	24.9	6.54

τ	ι	i	τ	ι	i
68	24.3	6.38	440	7.58	1.987
70	23.8	6.24	460	7.44	1.955
72	23.3	6.11	480	7.31	1.920
74	22.9	6.01	500	7.19	1.889
76	22.4	5.88	600	6.72	1.768
78	22.0	5.77	700	6.40	1.682
80	21.6	5.66	800	6.17	1.622
82	21.2	5.56	900	6.00	1.578
84	20.9	5.49	1000	5.89	1.545
86	20.5	5.38	1200	5.71	1.500
88	20.2	5.30	1400	5.61	1.475
90	19.8	5.20	1600	5.55	1.460
92	19.5	5.11	1800	5.51	1.450
94	19.2	5.04	2000	5.49	1.442
96	18.9	4.96	2200	5.49	1.441
98	18.7	4.91	2400	5.49	1.442
100	18.4	4.83	2600	5.50	1.446
120	16.2	4.25	2800	5.51	1.450
140	14.5	3.80	3000	5.53	1.453
160	13.3	3.49	3200	5.54	1.459
180	12.3	3.23	3400	5.56	1.461
200	11.5	3.02	3600	5.58	1.467
220	10.9	2.86	3800	5.60	1.471
240	10.3	2.70	4000	5.62	1.478
260	9.88	2.60	5000	5.72	1.502
280	9.48	2.49	6000	5.82	1.530
300	9.13	2.40	7000	5.91	1.552
320	8.83	2.32	8000	5.99	1.573
340	8.56	2.25	9000	6.06	1.592
360	8.32	2.18	10,000	6.13	1.610
380	8.11	2.13	20,000	6.59	1.730
400	7.91	2.08	30,000	6.86	1.803
420	7.74	2.03			

[a] In this book particle energy-loss rates are measured in energy units per unit distance, or energy units per unit areal density.

[b] τ is in Mev, ι in Mev/cm, and i in Mev gm^{-1} cm^2.

was found from measured particle ranges (B-T 58) by using the calculated correction, and weighting most strongly the measurements for which the correction was not important. In this way a mean ionization potential, $I = 331 \pm 6$ ev, was found. For protons of energy above 40 Mev the computed rate of energy loss is consistent with these experimental data. At somewhat lower velocities, where the detailed